

1 **Design and simulations of Refrigerated Sea Water Chillers with CO₂ ejector pumps for**
2 **marine applications in hot climates**

3
4 **Jakub Bodys^(a), Armin Hafner^(b), Krzysztof Banasiak^(c),**
5 **Jacek Smolka^(a), Yves Ladam^(d)**

6 ^(a) Institute of Thermal Technology (ITT), Silesian University of Technology (SUT),
7 Gliwice, 44-100, Poland, jakub.bodys@polsl.pl

8 ^(b) Norwegian University of Science and Technology,
9 Trondheim, 7465, Norway, armin.hafner@ntnu.no

10 ^(c) SINTEF Energy Research,
11 Trondheim, 7465, Norway, krzysztof.banasiak@sintef.no

12 ^(d) Kuldeteknisk AS,
13 Tromsø, 9010, Norway, yves@kuldeteknisk.no

14
15 **Abstract**

16 Various system configurations have been developed to improve the R744 systems under hot
17 ambient conditions. However, stationary land applications are characterised by negligible limits
18 on space for system equipment, unlike the marine industry, i.e. on-board fishing vessels. The
19 baseline CO₂ refrigeration system for fishing vessels was developed by a cooperating industrial
20 company, namely the Refrigerated Sea Water Chillers operation on the Norwegian coast, which
21 confirmed the successful application of this approach. In this study, modified layouts are
22 evaluated for operation in warmer climates without the need for an additional compressor unit,
23 thus maintaining the compactness of the unit. Flash gas valve-, parallel compression- and multi-
24 ejector systems were numerically investigated including ejectors section and flooded
25 evaporator. Sea water temperatures as occurring in Mediterranean and East-Asian waters were
26 investigated. Both the optimal high-pressure as well as the pressure level in an intermediate
27 pressure receiver were controlled to achieve low energy consumptions. Finally, an up to 70%
28 performance improvement was obtained in the case of the most advanced installation working
29 in warm East-Asian waters. The obtained results showed that the proper design of the system
30 should ensure no necessity for an additional compressor in warmer climates while still
31 maintaining the designed cooling capacity.

32 **Keywords**

33 R744, CO₂, multi-ejector system, marine application, efficiency improvement

34 **Nomenclature**

35 Acronyms and abbreviations

36 GWP Global Warming Potential

37 ODP Ozone Depletion Potential

38 R717 Ammonia

39 HC Hydrocarbons

40 R744 Carbon-dioxide

41 TFA Trifluoroacetic acids

42	HF	Hydrogen fluoride
43	R1234yf	Tetrafluoropropene
44	HFC	Hydrofluorocarbons
45	HFO	Hydrofluoroolefins
46	R134a	Tetrafluoroethane
47	VRC	Volumetric Refrigeration Capacity
48	COP	Coefficient of Performance
49	IHX	Internal Heat Exchanger
50	LPR	Low Pressure Receiver
51	MER	Mass Entrainment Ratio
52	SN	Suction Nozzle
53	MN	Motive Nozzle
54	IPR	Intermediate Pressure Receiver
55	SST	Sea Surface Temperature
56	NEO	NASA Earth Observation
57	EES	Engineering Equation Solver
58	IP	Intermediate Pressure
59		
60	Roman Letters	
61	p	pressure, <i>bar</i>
62	h	specific enthalpy, $kJ\ kg^{-1}$
63	s	specific entropy, $kJ\ kg^{-1}\ K^{-1}$
64	\dot{m}	mass flow rate, $kg\ s^{-1}$
65		
66	Greek Letters	
67	χ	Mass Entrainment Ratio, -
68	η	Efficiency, %
69		
70	Subscripts	
71	in	Ejector inlet
72	out	Ejector outlet
73	is	Isentropic
74	mn	Motive nozzle
75	sn	Suction nozzle
76	COMP	Compressor
77	EVAP	Evaporator
78	DIF	Diffuser outlet
79	VALVE	Expansion valve
80	MOT	Motive nozzle port
81	FGAS	Flash gas
82	LPR	Lower Pressure Receiver
83	PAR	Parallel compressor
84	BASE	Base compressor
85		

86 1. Introduction

87 According to the first turn in global trends of refrigerants presented by the Montreal [1] and
88 Kyoto [2] protocols, the next steps toward the direction of environmentally friendly working
89 fluids have already been undertaken. According to Global Warming Potential (GWP) and
90 Ozone Depletion Potential (ODP), regulations presented by European Commission [3] ensure
91 no limits for natural working fluids such as ammonia (NH₃, R717), hydrocarbons (HC) or
92 carbon-dioxide (CO₂, R744). According to the listed natural refrigerants, the last ensures many
93 additional advantages besides global environment safety. When applying R744, local safety
94 during exploitation and transport is provided by its non-toxic, non-flammable characteristics
95 and, as a consequence, the least stringent safety class, A1, is achieved [4]. It is worth noting
96 that both safety ranges should be satisfied - global and local. Meanwhile, produced synthetic
97 refrigerants characterised by very low GWP values might simultaneously have serious
98 disadvantages. Namely, the decomposition processes (with or without fires) of these ultra-low
99 GWP synthetic refrigerants result in toxic products such as trifluoroacetic acids (TFA) or
100 hydrogen fluoride (HF), which pose real dangers to human health in closed spaces such as
101 garages and ships [5]. On the other hand, refrigerants from the R1234 family are characterised
102 by safety class A2/L, for which the potential for safe servicing and maintenance have been
103 confirmed [6]. An analysis of alternative mixtures based on hydrofluorocarbons (HFC) and
104 unsaturated HFCs to substitute for high GWP refrigerants has been provided as well [7].
105 Nevertheless, this study presents a comparison of economic benefits that shows that R744 is a
106 more efficient solution than systems applying the mixtures mentioned.

107 Economic and technical aspects of R744 application provide the same positive perspective as
108 the aforementioned environmental factors and legal regulations. This is due to the
109 thermodynamic properties of R744, which result in high performance operation in real cycles
110 [8]. First, the levels of high- and low-pressure sides provide lower pressure ratios than
111 traditional halocarbons. Consequently, a higher efficiency of compressor operation is provided
112 [9] [10]. In addition to lower pressure ratios, the pressure values in R744 systems are higher
113 than in classical units using tetrafluoroethane (R134a). This provides for a lower specific
114 volume and smaller size compressors - and further lowers investment costs [9], [11]. Moreover,
115 smaller sizes of heat exchangers can be obtained according to relatively high volumetric
116 refrigeration capacity (VRC) and high heat transfer coefficients in CO₂ flows. Next, very low
117 temperature drops with corresponding pressure drops in installations allow designing smaller
118 piping systems with higher velocities of flowing working fluids. These features can be
119 summarized by the compact sizes of R744 installations and their high performance in operation
120 [11].

121 The described thermodynamic and ecologic features find application in fishing vessel
122 refrigeration units, where cooling of a catch during transportation is one of the crucial factors
123 of final fish quality and achievable prices. Nevertheless, the quantity of catch is important for
124 economic balance as well. Due to this, the refrigeration unit and its equipment should concern
125 machinery space limitations and maximum refrigerated storage space. Hence, the
126 aforementioned compact sizing and satisfactory performance have allowed the development of
127 refrigeration units for fishing vessels applications. Such installations have been developed by
128 Kuldeteknisk AS for new marine applications applying R744 refrigeration units. The catch is

129 cooled by Refrigerated Sea Water (RSW) Chillers, in which storage tank water temperature is
130 maintained at a level of $-1\text{ }^{\circ}\text{C}$. In Scandinavian ambient conditions, where heat rejection is
131 ensured by relatively cold sea water ($5\text{-}12\text{ }^{\circ}\text{C}$), such operations result in high performances of
132 the refrigeration units without sacrificing large amounts of space for the installation of the main
133 components. Regarding performance and the ecological aspects related to the green label of
134 R744, many of these installations are currently found in Norwegian fishing vessels.

135 Nevertheless, besides the mentioned advantages, some challenging areas have to be taken into
136 account for the process of further development. One such challenge is operation under high
137 ambient conditions such as off the southern Mediterranean coast or in Indonesian climates, the
138 reasons for which are related to the thermodynamic properties of R744. Namely, the relatively
139 low temperature of the critical point ($30.98\text{ }^{\circ}\text{C}$) [12] enforces the cycle to operate in transcritical
140 mode. In addition, the transcritical mode results in high expansion losses, which affect system
141 Coefficient of Performance (COP) in a negative way [9] [11]. Hence, more advanced solutions
142 have to be utilised in the case of R744 refrigeration units.

143 To maintain the applicability of the RSW system and its advantages in hot climates such as in
144 south Europe or Asia, some improvements could be introduced to the CO_2 refrigeration cycle.
145 The literature reports several studies in which the positive influences of various components
146 configurations were described. These solutions were developed on the basis of other CO_2
147 applications such as supermarket heating and cooling systems [13] [14] [15], mobile
148 refrigeration units [16] and residential heat pumps [17] [18].

149 The fundamental modification of the R744 system is based on the introduction of an
150 intermediate pressure receiver, which is sometimes called a liquid receiver. The potential
151 energy savings of this solution were described in the work of Gullo [19]. The author
152 theoretically analysed a refrigeration system for supermarket applications in three cities
153 characterised by high year-averaged temperatures - Rome (Italy), Valencia (Spain) and Seville
154 (Spain). The investigation showed up to a 9.6 % COP improvement in a combined case with
155 evaporator overfeeding and a parallel compression mode in comparison with a cycle based on
156 refrigerant R404A. In the work of Carvalho [20], the investment cost of liquid receiver and
157 additional equipment was evaluated to be high with regard to the obtained performance
158 improvement. On the other hand, the compact sizing for CO_2 showed potential for application
159 with small units of 1 kW power. Similar challenges in the investment cost area are related to
160 the mentioned HFO working fluids, thus most initial applications are focused on Mobile Air
161 Conditioning and small domestic refrigerators [21]. The higher performance of an R744 system
162 was presented by Sarkar [22], but a larger installation was analysed. The authors investigated
163 various configurations based on the parallel compression idea. In the case of the most promising
164 parallel compression with economiser, the COP increment was equal to 47.3 %. Cases of
165 smaller temperature differences resulted in COP improvements on the level of 15 %. Further
166 possibilities for system improvement are related to proper integration of heating and cooling
167 functions. A fully integrated building design process becomes a standard indicator of a well-
168 planned state-of-the-art investment [23]. An energy savings based on an integration of
169 transcritical CO_2 and desalination systems was reported in the work of Farsi et al. [24]. In the
170 work of Manjunath et al. [25], waste heat from shipboard gas turbines was utilised for heating
171 purposes as well as to provide a power supply for a transcritical CO_2 refrigeration unit. Another

172 cogeneration approach based on carbon dioxide was reported in the paper presented by Akbari
173 and Mahmoudi [26]. Those authors presented promising results of a supercritical Brayton and
174 transcritical refrigeration cycle integration. The analysis showed benefits in the form of energy
175 savings and optimised unit-cost production.

176 In addition to the heat recovery approach, work recovery of expansion losses is a perspective
177 way to improve unit COP. The aforementioned expansion losses could be described as having
178 a large potential for work recovery in the R744 system [11]. Direct and indirect work recovery
179 for the expansion process was described as having yielded satisfactory results. However, direct
180 solutions in the form of gear expanders or turbines could be described as having less demand
181 in mobile units according to reliability. The mentioned reliability can be provided by devices
182 with no moving parts and simple construction. Such features are delivered by introducing
183 ejectors into transcritical CO₂ refrigeration systems [27]. The recovered work could be received
184 in two ways regarding actual needs. The ejector operation can be focused on the pressure
185 increment before the suction ports of compressors, resulting in lower energy demand. On the
186 other hand, the ejector provides a pumping effect and recirculation of liquid CO₂, resulting in a
187 lower mass flow rate through the compressor section. In consequence, it provides lower
188 compressor work. Potential for highly-efficient operation was indicated in the work of Bai et
189 al. [28], where an advanced exergy analysis on a transcritical R744 ejector system was
190 presented. A developed decomposition of exergy destruction sources has shown that up to 43.44
191 % of exergy destruction could be avoided. The most significant component was the compressor
192 and next ejector. Hence, a substantial improvement buffer can still be developed. A similar
193 system configuration was studied by Zhu et al. [29]; nevertheless, those authors used
194 experimental methods and were concerned with the influence of ejector performance on overall
195 system COP. Moreover, developed coefficients allowed for an analysis of other system
196 components' states, i.e. that of the liquid separator. Interesting results were provided by Zheng
197 et al. [30], who utilized a dynamic simulation of a transcritical R744 ejector system. Those
198 authors introduced a two-stage evaporator integrated with the ejector, obtaining increased
199 functionality and better performance in the transient states of the system.

200 An experimental comparison provided by Lucas showed a 17 % COP improvement due to the
201 ejector implementation [31]. The authors investigated the influence of the high pressure side on
202 ejector and overall system performances. The range of investigated gas cooler temperatures was
203 constrained from 30 °C to 40 °C, whereas the evaporation temperatures were between -10 °C
204 and -1 °C. The COP improvement showed good potential for R744 transcritical system
205 operation under relatively high ambient conditions. According to the described ejector solution,
206 fully developed solutions were presented for applications such as in supermarket refrigeration
207 systems [13]. The authors described the idea of parallel working ejectors to cover various
208 system loads with simultaneously high efficiency for these devices. Several authors
209 investigated this solution based on a multi-ejector block. A performance mapping of a multi-
210 ejector block was delivered on the basis of laboratory tests and described in the work of
211 Banasiak [32]. The presented results of the block performance throughout the wide range of
212 operating conditions characteristic of supermarket operations delivered a range of efficiencies
213 that were a function of pressure ratio (the outlet to the suction pressure) and motive pressure.
214 Depending on the mentioned parameters, the efficiency ranged from 12 % to 33 % for a pressure

215 ratio of 1.1 and 75 bar and a pressure ratio of 1.3 and 95 bar, respectively. The mentioned multi-
216 ejector block efficiency can be described by the same function as that for a single ejector,
217 according to the definition used [33]. Further analysis of a global multi-ejector system was
218 provided by Haida [34]. The authors described the comparison of PC and multi-ejector system
219 performances in a laboratory test rig based on high ambient temperatures. The obtained results
220 showed up to 8 % system COP improvement when operating in the multi-ejector mode.
221 Numerical analyses of multi-ejector block performance were performed in cooperation with the
222 authors of the mentioned experimental tests [35]. According to those results, an even higher
223 efficiency of 38 % could be obtained when pressure drops in collectors are reduced. Moreover,
224 the first studies on multi-ejector implementation to a heat pump system were provided as well
225 [36]. Having regarded that the concept of this device was planned for refrigeration applications
226 [13], it could be said that constant development of this technology is visible.

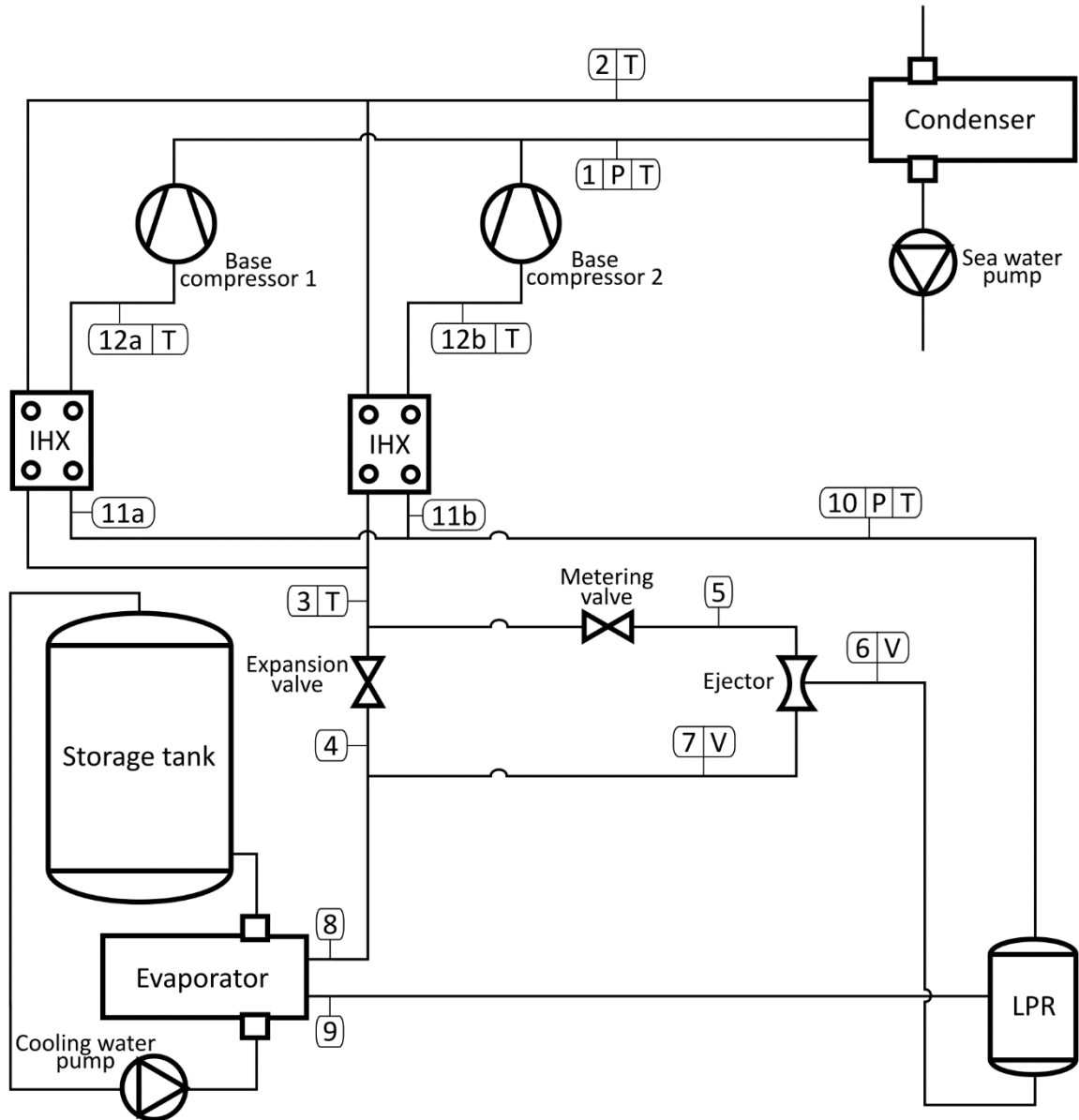
227 In this study, an investigation of a modified RSW installation for fishing vessels operating under
228 high ambient conditions is provided. To the best of the authors' knowledge, a study of the R744
229 installation for fishing vessels with constrained machinery room space is not provided in the
230 literature. The baseline case with a liquid ejector designed for Scandinavian conditions was
231 simulated on the basis of a developed mathematical model and measurement data from an actual
232 working RSW installation (Kuldeteknisk AS, Tromsø). Highly efficient operation of the
233 actually operating unit on the northern Norwegian coast was confirmed. To investigate system
234 performance under high ambient conditions, the developed baseline model was modified by
235 introducing an intermediate pressure receiver and parallel compression of the flash gas.
236 Moreover, an additional model of a multi-ejector system was developed and simulated as well.
237 On the basis of satellite data, Mediterranean and East-Asian water temperatures were chosen as
238 representative of high-temperature climates. Parameterisation of the operating conditions
239 delivered data on the most efficient system operation. Simulated configurations were compared
240 in the light of the system COP and space requirements. Additional equipment was analysed and
241 is discussed to propose the best solution with regard to performance and necessary
242 modifications for each of the analysed climates. Finally, the relation between multi-ejector
243 module efficiency and system performance is discussed. The overall conclusions on the most
244 promising modification of RSW installation are stated.

245 **2. Refrigerated Sea Water installation**

246 **2.1. Scandinavian operation - Baseline System**

247 The Baseline System of the analysed RSW installation is presented in Fig. 1. Similar
248 installations are used on fishing vessels in the region of northern Norway. This CO₂ cycle is
249 built on the basis of the cycle proposed by Gustav Lorentzen [11]; nevertheless, a liquid ejector
250 was implemented as an additional component. Additional control and measurement equipment
251 is marked by frames with proper letters, where T is temperature measurement, P is pressure
252 measurement, and V is flow measurement. Moreover, in Fig. 1, state points used in further
253 calculations are marked. Operation of the installation is focused on cooling the water from a
254 storage tank loop, where the set-point temperature of the water is approximately
255 -1 °C. Heat rejection is ensured by a sea water supplied condenser. Scandinavian conditions
256 ensure water inlet temperatures usually below 10 °C. The analysed installation is equipped with

257 two compressors with a maximum electrical power consumption equal to 44 kW each at 34.85
258 bar of evaporation pressure and 10 K superheating [37]. The suction gas is supplied from
259 internal heat exchangers (IHX) separately for each compressor. Evaporator load varies
260 depending on water storage tank load and share of fresh water. From the refrigerant side, the
261 evaporator is supplied by a stream expanded in a throttling valve and the ejector. The
262 aforementioned ejector ensures liquid circulation between a low pressure receiver (LPR) and
263 the evaporator. Finally, according to the collaboration with the Kuldeteknisk AS, some data of
264 the system components used in the study had confidential character. Due to the mentioned
265 collaboration, the comprehensive analysis of the considered refrigeration system was available.
266 In general, classic oil recovery from the low-pressure side was adjusted in order to meet the
267 pressure in low-pressure receiver. Next, the oil was pumped back into the oil separators nearby
268 the compressors section. Generally, the auxiliary oil-receiving loop is built by high-pressure
269 side separator and the receivers installed together with the CO₂ tanks. A system using this
270 approach was described by Haida et al. 2016 [34]. Moreover, the literature reports that in the
271 case of heat transfer, integrated lubricant-R744 tanks allows for improved heat transfer. In
272 consequence there is a possibility to minimize the lubricant leakage [38].



273

274

275

Figure 1. Baseline RSW chillers - R744 refrigeration unit installed in a fishing vessel operating under Scandinavian conditions.

276

277

278

279

280

281

282

283

284

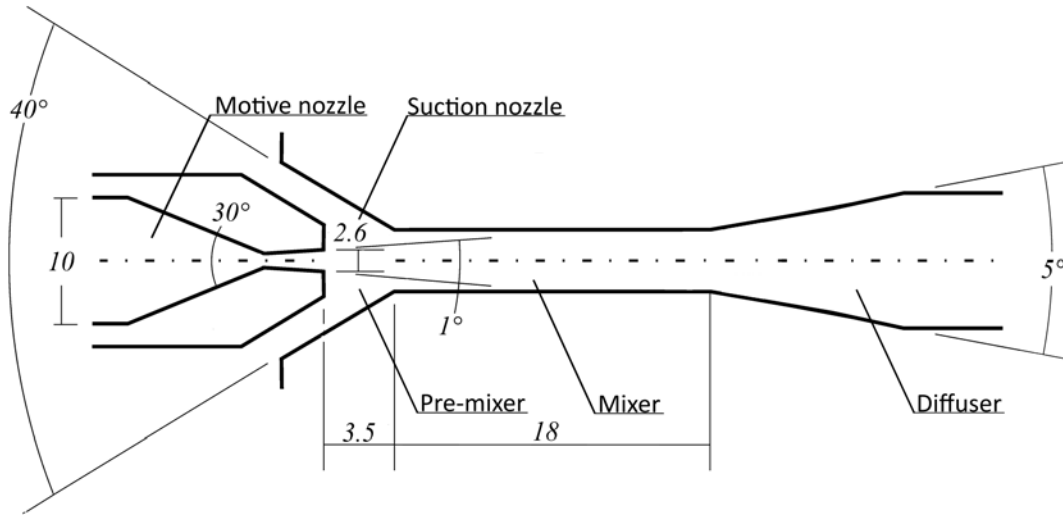
285

286

287

Operation of the mentioned liquid ejector in the analysed RSW installation is focused on the internal circulation of liquid. Energy required for this circulation is recovered from expansion losses on the basis of the ejector work principle. Namely, a flow of subcooled R744 from the IHX is divided into two streams at point 3 (see Fig. 1). One stream is directly expanded in the throttling valve, and the second stream flows through the ejector. The basic scheme of the ejector geometry is presented in Fig. 2, where a motive nozzle, suction nozzle, pre-mixing chamber, mixer and diffuser are schematically shown. The mentioned high pressure subcooled motive stream is expanded in the motive nozzle and converted to a high velocity flow in the premixing chamber. The expansion process in the motive nozzle reaches pressures below that of the suction nozzle port, hence a suction phenomenon occurs. Next, the pressure of the mixed motive and suction streams is increased in the diffuser. Nevertheless, phenomena of the suction and pressure lift are related to each other. Moreover, ejector operation results in only one of the

288 mentioned phenomena being characterised by high intensity, and in the second becomes
 289 simultaneously minor. Thus, obtaining high values of suction stream mass flow rate are related
 290 to low values of pressure difference (pressure lifts) between the suction and the outlet ports. In
 291 the case of the presented RSW installation, the ejector ensures circulation of the liquid, where
 292 the goal of its operation is given by the high mass flow rate of the suction stream. Such an
 293 operation results in smaller mass flows through the compressors. On this basis, system COP is
 294 improved in comparison with that of the traditional cycle without the ejector.



295

296

Figure 2. Liquid ejector geometry scheme with the marked flow sections.

297

2.2. Efficiency of ejector operation

298

299

300

301

302

303

For this study, the ejector efficiency definition (Eq. 1) presented by Elbel and Hrnjak [33] was used. The efficiency of the ejector is given as a ratio between recovered work and maximum available work delivered in the motive nozzle. Namely, the numerator is defined as a difference of enthalpies obtained from an isentropic and isenthalpic compression process from the suction nozzle pressure to the ejector outlet pressure. In the second part, the numerator is defined similarly but considers the expansion process in the motive nozzle:

304

$$\eta_{EJ} = \chi \cdot \frac{h_{|s=SN,in} p=p_{out} - h_{SN,in}}{h_{MN,in} - h_{|s=MN,in} p=p_{out}}, \quad (1)$$

305

306

307

308

where h is the specific enthalpy, subscript s represents the specific entropy in the suction nozzle (SN) and the motive nozzle (MN), p is the pressure, and in and out are the ejector inlets and outlet, respectively. In this definition, parameter χ , which is called mass entrainment ratio (MER), is used (Eq. 2):

309

$$\chi = \frac{\dot{m}_{SN}}{\dot{m}_{MN}}, \quad (2)$$

310

where \dot{m} is the mass flow rate.

311

3. RSW system at high ambient temperatures

312

3.1. Warm waters of the Mediterranean and East-Asian regions

313

314

The challenging matter of higher heat rejection temperatures should be solved to maintain aspects of high performance and economy. It is worth noting that even seas located in northern

315 conditions report rising temperature levels. An example is given on the basis of satellite data
316 and analysis focused on the basin of Gulf of Finland (Baltic Sea) [39]. In this region, the average
317 annual SST in 1982 was 6.8 °C. Due to the significantly visible warming of approximately 0.04
318 K per year, the mentioned value increased to 8.2 °C in 2014. However, the temperature change
319 was not constant, i.e., in the middle of the 1980s, the temperature dropped to 5.0 °C, and noting
320 a significant increase up to 7.3 °C in 1989. In the more global case of the Mediterranean Sea, a
321 similar increasing trend has been described [40]. An interesting fact of the same kind as in the
322 Gulf of Finland, an increasing temperature rate of 0.4 K per decade in the last 30 years was
323 observed. Moreover, simulation predictions based on data from the period 1986-2015 showed
324 an approximately 5.8 K increment in the average SST at the end of XXI century.

325 **3.2. Constraints according to fishing vessel construction**

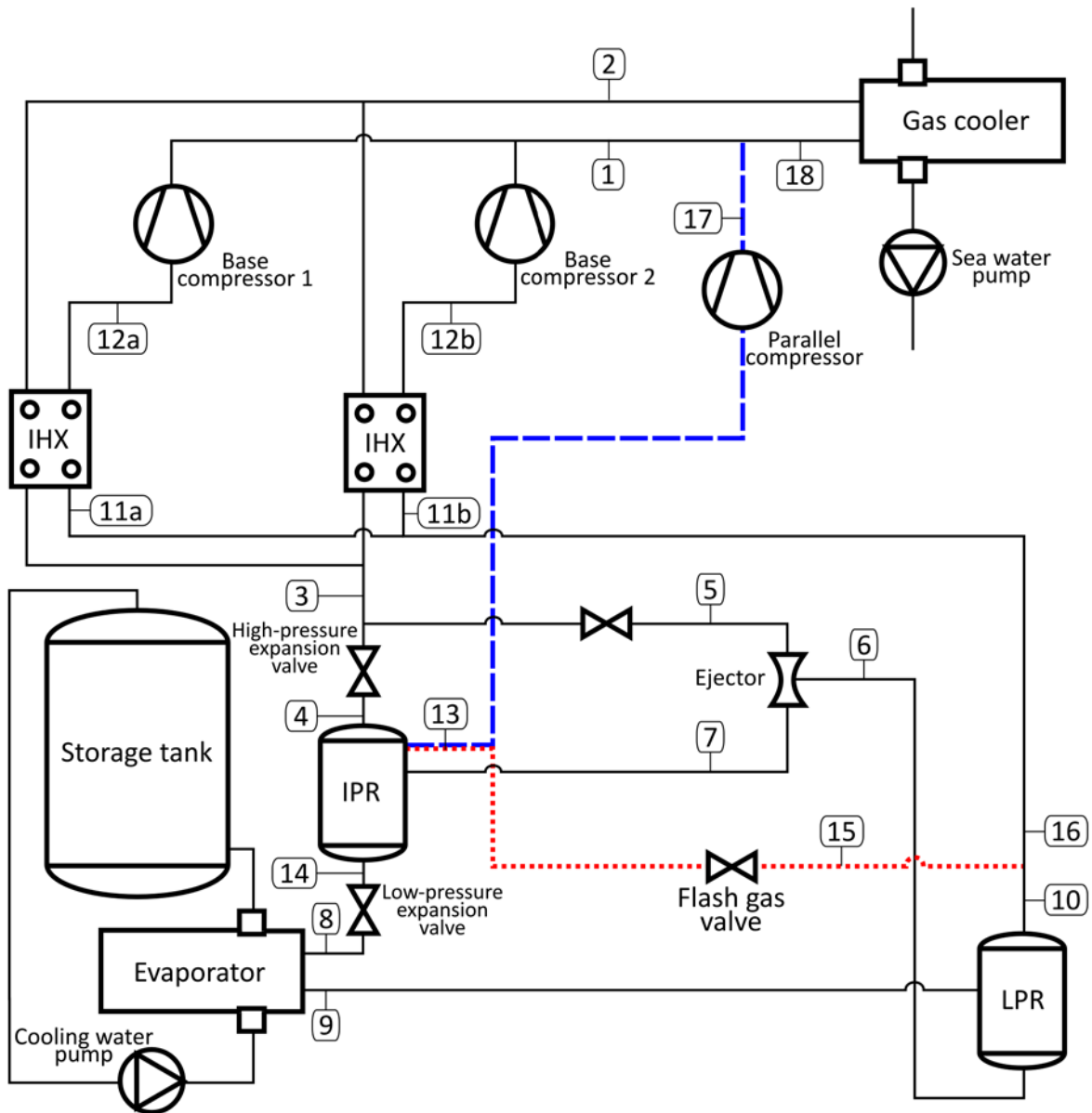
326 Higher temperature differences between ambient and cooled media usually require increased
327 power consumption and larger refrigeration unit sizes. The R744 RSW unit provides a solution
328 in the form of the overall compact size of the installation. However, analysis of power
329 consumption increases and compressor size should allow further economic analysis of such an
330 implementation to fishing vessels according to available space in the machinery room.
331 Constrained space for system modifications and enlargement could be described as a one of the
332 challenges in such an application.

333 **3.3. Analysed modifications to the Baseline System**

334 The motivation for introducing the RSW for hot climate waters is concentrated on the compact
335 size of the system and the ecological label assigned to the natural refrigerant. However, the
336 challenge of heat rejection at higher sea water temperatures has to be solved to maintain the
337 performance and economic aspects. Meanwhile, the temperatures on the Mediterranean coast
338 and in the south-east region of Asia vary from 18 °C to 21 °C and from 30 °C to 33 °C,
339 respectively. According to Sea Surface Temperature (SST) data available in NASA Earth
340 Observation (NEO) databases, the waters of the mentioned East-Asian regions can even reach
341 35 °C [41]. In the region of the Mediterranean Sea, the temperature differences in comparison
342 to the baseline north conditions are smaller. Nevertheless, water temperatures reach up to 23
343 °C [41]. The R744 RSW unit is a compact installation. However, analysis of power
344 consumption increases and compressor size should allow further economic analyses of such an
345 implementation on fishing vessels according to the available spaces in their machinery rooms.
346 The constrained spaces available for system modifications and enlargement could be described
347 as a one of the challenges in such applications.

348 According to the above described space constraints and simultaneous higher power demands,
349 the configurations of ejector-, flash gas- and parallel compression- units were analysed without
350 modification to the rest of the Baseline System installation (black lines). In Fig. 3, the scheme
351 of the modified Baseline System model (red dotted and blue dashed lines) is presented. An
352 Intermediate Pressure Receiver (IPR) was introduced with a second low-pressure expansion
353 valve for liquid expansion. Flash gas (red dotted line) is expanded via the flash gas valve and
354 then mixed with the refrigerant stream from Lower Pressure Receiver (LPR). The parallel
355 compressor line (blue dashed line) was separated from the flash gas line and directed to main
356 line leading to the gas cooler. To simulate hot climate conditions, higher heat rejection

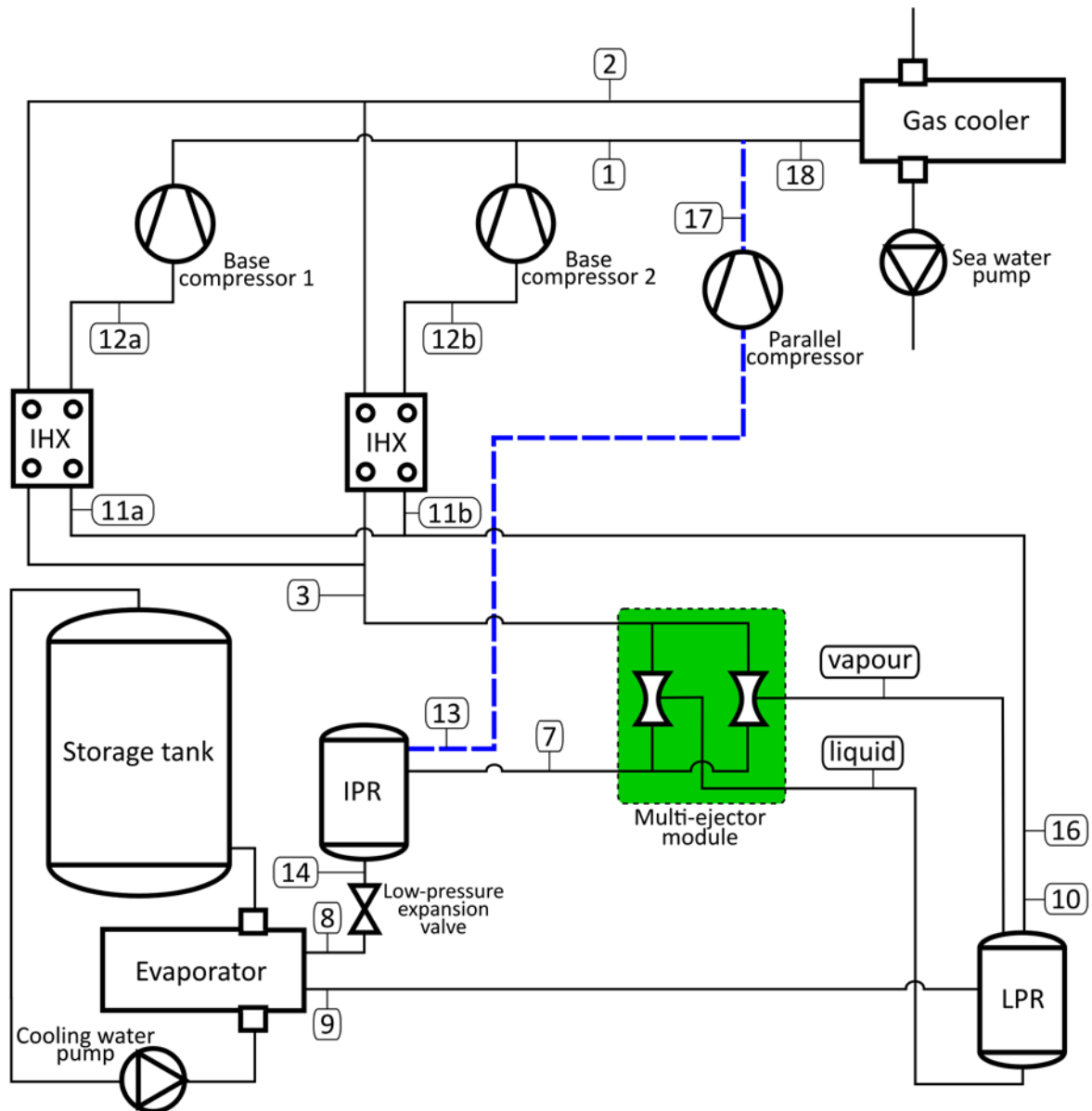
357 temperatures were assumed. To analyse the energy demands of the RSW unit at various fishing
 358 vessel locations, two temperature levels were taken into consideration. Hence, temperatures of
 359 21 °C and 33 °C characteristic of the Mediterranean Sea and the waters of east Asia,
 360 respectively, were assumed [41]. To investigate the influence of each modification, two systems
 361 were simulated separately. The first system was based on flash gas expansion (FGV), for which
 362 the entire amount of flash gas was directed to the flash gas valve. Therefore, when the FGV
 363 mode was tested, the parallel compression line was turned off. The second system was based
 364 on parallel compressor utilisation (PC). In that mode, the flash gas valve was closed, and the
 365 entire flash gas stream was drawn in by the parallel compressor.



366
 367 Figure 3. Modified RSW installation with introduced additional equipment: IPR, flash gas
 368 line (red dotted) and parallel compression line (blue dashed).

369 On the basis of the presented FGV and PC installations, the next generation of R744 was
 370 developed and described in the literature [13]. Namely, the throttling valve was exchanged with

371 an ejector device, which served as a basis for further cycle improvement, and such an
372 installation is presented in Fig. 4. The basis of this modification is related to the fact that the
373 ejector motive nozzle provides similar mass flow rates as during expansion in a throttling valve.
374 Moreover, to maintain the compact sizing and improve system reliability, ejectors were
375 connected in a multi-ejector module to form one compressed device (green frame in Fig. 4).
376 Each ejector is controlled by individual valves. Due to this, overall regulation is based on the
377 binary idea of opened and closed fixed geometry ejectors working in a parallel mode. The
378 concept of such an approach was delivered in the work of Hafner [13]. The same idea was
379 investigated in this study through simulation of a separated multi-ejector system (ME). The
380 module work is utilised to pump working fluid from the LPR to the IPR. The operation of the
381 vapour ejectors in the multi-ejector module provides unloading of the base compressors by
382 sucking vapour produced in the evaporator to the higher pressure of the IPR, and high enough
383 ejector performance and sufficient motive mass flow rates allow drawing the entire evaporator
384 stream. Eliminating the base compressor and operating with parallel compressors only would
385 be a potential solution for RSW implementation.

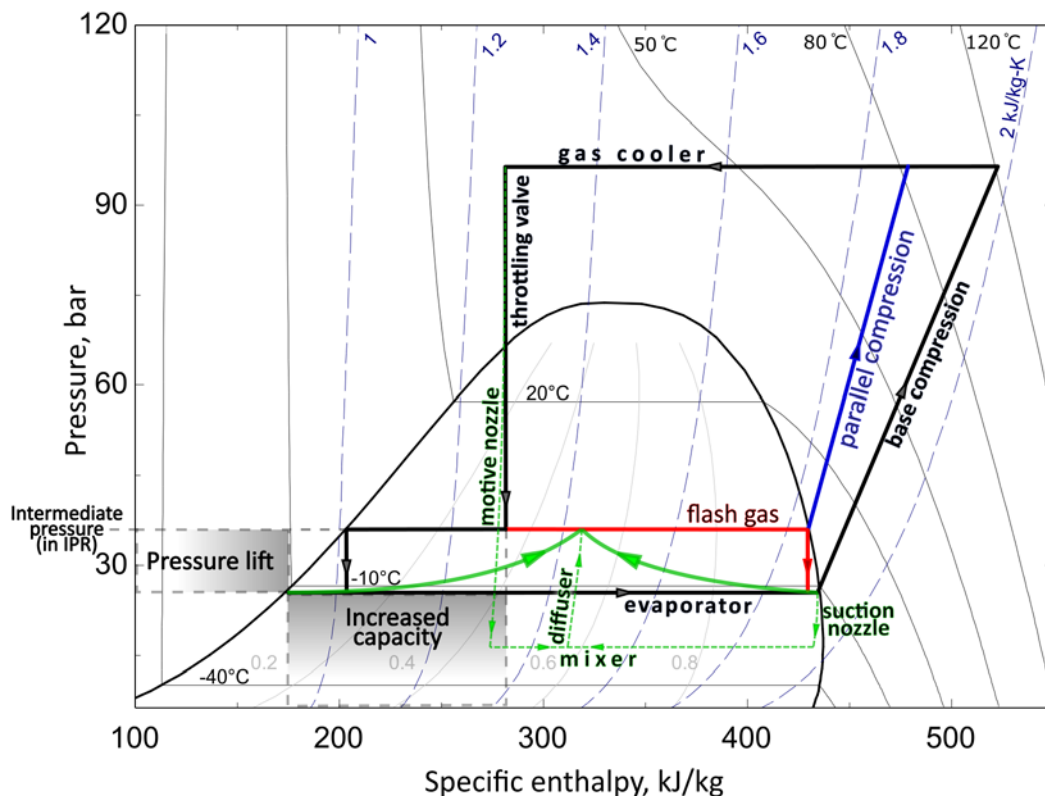


386

387 Figure 4. Concept of a new RSW installation based on parallel working ejectors contained in
 388 a multi-ejector module.

389 The main components of the layouts mentioned were presented on the pressure-enthalpy
 390 diagram of R744 in Fig. 5. In order to maintain a clarity, the colours used for the representation
 391 of each modification correspond to the colours used in Fig. 3 and Fig. 4 – red is FGV, blue is
 392 PC and green is ME. Moreover, the processes of each ejector section were marked by green
 393 dashed lines. In the ME system, the throttling of the high-pressure refrigerant is exchanged to
 394 expansion in the motive nozzle, the expansion ends below the evaporator pressure what results
 395 in the entrainment via the suction nozzle (vapour suction illustrated in Fig. 5). After mixing of
 396 the primary and secondary streams in the mixer, the pressure is lifted in the diffuser up to the
 397 IPR level. From the point of view of the system performance, an introduction of the ejectors
 398 benefits in the pressure lift between the evaporator and IPR. In a consequence, the parallel
 399 compressor operates with higher suction pressure and the lower pressure ratio what results in
 400 the reduced input power. Next, the advantageous approach of the evaporator flooded operation

401 and proper adjustment of the intermediate pressure allows for increased cooling capacity.
 402 Finally in Fig. 5, the clearly visible technical advantages of R744 as the working fluid can be
 403 discussed as well. Firstly, the low pressure ratio in the range from 1.5 to 4 could be characterised
 404 as substantially lower than that for the synthetic refrigerants. The result of such a value is
 405 obtained at the higher efficiency of the R744 compressors. Next, consideration of high
 406 operational pressures more than 30 bar leads to other advantageous properties such as low
 407 specific volume and more compact sizes of heat exchangers and compressors. Moreover, small
 408 pressure drops (and consequently very low temperature drops) in CO₂ installations allow for
 409 the selection of the smaller piping systems what again leads to the compact sizing – very
 410 demanded from the marine industry.

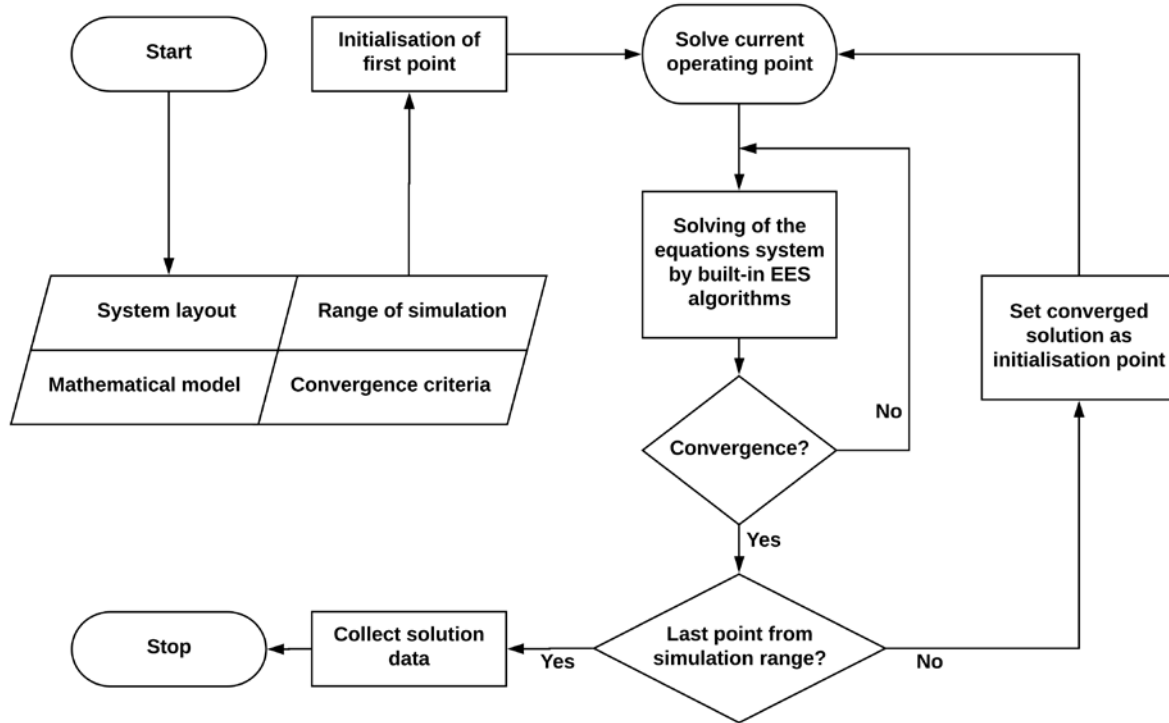


411
 412 Figure 5. Representation of the modified system layouts (red is FGV, blue is PC and green is
 413 ME).

414 4. R744 cycle modelling - Baseline and modified configurations

415 The utilised computational approach was presented in the form of flowchart in Fig. 6. The
 416 system layout and corresponding mathematical model constituted the first step. The points used
 417 in the stream formulations are presented in Figs. 1, 3 and 4. A real fluid property library
 418 available in the employed software was used for the determination of the thermodynamic
 419 parameters at a given system point. Next, the convergence criteria and range of simulation were
 420 established for the given system configuration. The convergence criteria were set to 10^{-5} for
 421 both relative residuals and maximum variable change. The authors found that the precise
 422 initialisation point is challenging but crucial for the final convergence of the obtained solution.
 423 A system of equations was implemented in the Engineering Equation Solver (EES) to iteratively
 424 solve each model [42]. This tool offers the Newton-Raphson method as a built-in default

425 solving algorithm for obtaining solutions of sets of non-linear equations. The solution obtained
 426 for the given operating point was utilised for the next point computations what substantially
 427 improved the convergence time. A series of calculations of firstly established range was
 428 finalised by data collection prepared for the further analysis.



429

430

Figure 6. Solving procedure presented in the form of flowchart.

431

4.1. Fundamentals of the mathematical modelling approach implemented in the Engineering Equation Solver

432

433 The developed Baseline model was based on the measurement data delivered by the fishing
 434 vessel operator. The model was used to evaluate the performance of the actual installation. To
 435 simulate higher operating conditions, the modified models were prepared. However, the models
 436 were developed on the basis of the Baseline model used for actual cycle evaluation. Namely,
 437 the analyses of the Baseline and modified RSW installations were executed on the basis of
 438 energy and mass balance equations. In the following formulations, point identification is based
 439 on the Baseline System (Fig. 1) and the modified system scheme (Figs. 3 and 4).

440 The compressors consume energy delivered to the systems. Hence, a total compressor power
 441 equation was formulated:

$$442 \quad \dot{W} = m_{COMP1} \cdot (h_1 - h_{12a}) + m_{COMP2} \cdot (h_1 - h_{12b}). \quad (3)$$

443 To calculate the energy distribution between the evaporator, ejector diffuser and expansion
 444 valve, the energy balance of this section is formulated in Eq. 4:

$$445 \quad \dot{m}_{EVAP} \cdot h_8 = \dot{m}_{DIF} \cdot h_7 + \dot{m}_{VALVE} \cdot h_4. \quad (4)$$

446 Mass stream balances from Eq. 3 and Eq. 4 were formulated to obtain distribution of mass flow
 447 through the evaporator, expansion valve and ejector motive nozzle:

448
$$\dot{m}_{COMP} = \dot{m}_{VALVE} + \dot{m}_{MOT}, \text{ and} \quad (5)$$

449
$$\dot{m}_{EVAP} = \dot{m}_{VALVE} + \dot{m}_{DIF}, \quad (6)$$

450 where \dot{W} is power, \dot{m} is mass flow rate, and h is specific enthalpy. The subscript COMP denotes
 451 the compressor, EVAP denotes the evaporator, DIF denotes the ejector outlet port, VALVE
 452 denotes the expansion valve, and MOT denotes the ejector motive port. In addition to the
 453 compressor power consumption, the evaluation of the compressor work was based on the
 454 equation for the compressors' isentropic efficiency (Eq. 7):

455
$$\eta_{is} = (h_{1,s} - h_{12}) / (h_1 - h_{12}), \quad (7)$$

456 where the subscript *is* denotes isentropic, and *s* is specific entropy. As a simulation result, the
 457 process mass flow rates of the system were calculated. Hence, calculation of the system power
 458 demand at given operating conditions and evaporator load was possible. Further, the system
 459 performance was presented in the form of the COP factor, which is defined as follows in Eq. 8:

460
$$COP = \frac{\dot{Q}_{EVAP}}{\dot{W}}, \quad (8)$$

461 where \dot{Q}_{EVAP} is the heat transferred in the evaporator. The equation of evaporator energy
 462 balance (Eq. 9) is formulated as

463
$$\dot{Q}_{EVAP} = \dot{m}_{EVAP} \cdot (h_9 - h_8). \quad (9)$$

464 The analysis of the flash gas valve and the parallel compression systems were based on the
 465 modified Baseline model. In the case of the flash gas valve, the introduction of the IPR, two
 466 expansion valves and an additional flash gas line was necessary. To model these modifications,
 467 the additional energy balance related to the IPR was formulated, as presented in Eq. 10:

468
$$\dot{m}_{VALVE} \cdot h_3 + \dot{m}_{DIF} \cdot h_7 = (\dot{m}_{EVAP} + \dot{m}_{FGAS}) \cdot h_{IPR}, \quad (10)$$

469 where subscript FGAS represents the flash gas, and IPR represents the intermediate pressure
 470 receiver. The vapour quality value in the IPR was estimated on the basis of the obtained IPR
 471 enthalpy and the assumed pressure in the tank. Moreover, the mixing of the flash gas stream
 472 and saturated vapour from LPR was modelled on the basis of mass (Eq. 11) and energy balance
 473 (Eq. 12):

474
$$\dot{m}_{FGAS} + \dot{m}_{LPR} = \dot{m}_{COMP}, \text{ and} \quad (11)$$

475
$$\dot{m}_{FGAS} \cdot h_{15} + \dot{m}_{LPR} \cdot h_{10} = \dot{m}_{COMP} \cdot h_{16}. \quad (12)$$

476 The parallel compression was related to the additional equation for compressor work (Eq. 13).
 477 The mixing of the base compressor stream and auxiliary compressor stream was modelled by
 478 the mass (Eq. 14) and energy (Eq. 15) balances:

479
$$\dot{W}_{PAR} = \dot{m}_{COMP,PAR} \cdot (h_{17} - h_{13}), \quad (13)$$

480
$$\dot{m}_{COMP,PAR} + \dot{m}_{COMP,BASE} = \dot{m}_{COMP}, \text{ and} \quad (14)$$

481
$$\dot{m}_{COMP,PAR} \cdot h_{17} + \dot{m}_{COMP,BASE} \cdot h_1 = \dot{m}_{COMP} \cdot h_{18}, \quad (15)$$

482 where the subscript $COMP_{PAR}$ represents the parallel compressor, and $COMP_{BASE}$ represents
483 the base compressor. Moreover, the separated isentropic efficiency equation (Eq. 16) for
484 parallel compression was added:

$$485 \quad \eta_{is,PAR} = (h_{17,s} - h_{13}) / (h_{17} - h_{13}), \quad (16)$$

486 where $\eta_{is,PAR}$ is the isentropic efficiency of the parallel compressor. Similarly, as in the baseline
487 simulations, the system COP was used as the evaluation factor. However, in the case of the
488 parallel compression, the work of the auxiliary compressor was included in the COP factor
489 defined in Eq. 17:

$$490 \quad COP = \frac{\dot{Q}_{EVAP}}{\dot{W} + \dot{W}_{PAR}}. \quad (17)$$

491 **4.2. Assumptions for the simulations of the modified systems**

492 According to the introduced devices, the following assumptions were provided for the flash
493 gas, parallel compression and multi-ejector systems.

494 Ejector operation was modelled on the basis of a 1-D homogeneous equilibrium model, in
495 which each section's efficiency and the pressure in the mixing section were assumed. The
496 efficiencies of the motive nozzle, suction nozzle and diffuser were assumed to be equal to 85
497 %, 80 % and 80 %, respectively, for both the vapour and liquid ejectors. Similar modelling
498 approach was presented by Liu and Groll [43] when slightly higher motive efficiency and
499 slightly lower diffuser efficiency were assumed. Moreover, similar results were obtained in the
500 other papers as well [44], [45]. Especially in the work of Liu and Groll [45] as well as the work
501 of Zhang et al. [46], the wide literature survey provided data of the efficiencies. In the work of
502 Ahammed [47], some conclusions listed by Liu and Groll [45] were used. The authors assumed
503 the constant mass entrainment ratio on the level of 0.85 [47]. Additional assumptions of
504 choked flow in the motive nozzle and constant pressure mixing section were introduced as in
505 this study [47]. Moreover, these results were validated with the experimental data presented by
506 Nakagawa [48]. The comparison resulted in some similarities between the simulated and
507 experimentally tested ejector performance simultaneously showing substantial discrepancies
508 between global factors of the system performance. After exergy analysis of the system
509 components, the exergy destruction of ejector components was substantially lower than in the
510 case of heat exchangers and compressor. Finally, the authors showed that the assumption of
511 ejector efficiency could be characterised as crucial having regard comparison of the ejectors.
512 On the other hand, it might have relatively larger margin in the case of whole system
513 comparison. Some additional examples of assumed ejectors efficiency can be found in more
514 recent paper of Zheng and Deng [49]. In that paper, the authors confirmed the most common
515 approach of the assumed isentropic efficiency value of 80 %. Moreover, the efficiency of the
516 motive nozzle was mostly higher than that of the mixer and diffuser and took values on the
517 level higher than 85 %. On the other hand, as presented in comprehensive review about ejector
518 refrigeration system modelling [50], the case of R744 is very specific because only few studies
519 linked the ejector model with the system modelling. In a consequence, the choice of the proper
520 model assumptions such as the ejector efficiency is still a challenging matter. Hence, the
521 assumptions of sections' efficiency in this study in range 80 % - 85 % could be characterised

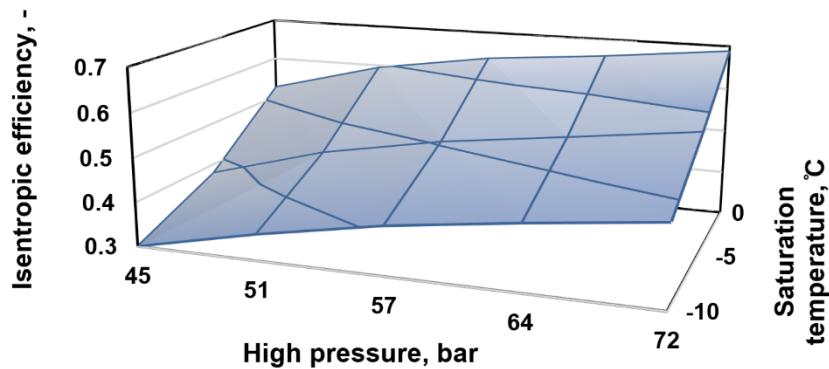
522 as typical but not the highest from the reports available in the literature. The assumed pressure
523 drop between the suction nozzle outlet and the mixer section was equal to 100 kPa on the basis
524 of the authors' previous experience [44]. In the Baseline System, pressure lift is utilised only
525 for the pressure drop between LPR tank and the evaporator, and thus the estimated ejector
526 efficiency was 1.15 %. Furthermore, the liquid ejectors in the case of the modified systems were
527 described by a constant overall efficiency equal to 15 %. This assumption was made for the
528 single liquid ejectors as well as the liquid ejectors section in the multi-ejector module.
529 According to the various pressure levels in the evaporator and IPR tank, the necessary motive
530 stream was calculated.

531 In the case of the ME system, two different approaches were used in the computational
532 procedure. According to the large amount of potential recovery work in the case of East-Asian
533 conditions, it was assumed that the ejector work would be enough to intake the entire evaporator
534 stream. This means zero power consumption by the base compressors. Due to that, the
535 necessary efficiency was calculated and is further analysed in the discussion of the results. The
536 evaluation of efficiency allows for the statement that this assumption was reasonable. Another
537 approach was provided in the case of the Mediterranean climate, for which potential recovered
538 work was lower. In this case, ejector efficiency was assumed to be a function ranging from 20
539 % to 35 % on the basis of performance maps presented in the work of Banasiak [32]. This
540 assumption provided results in the form of evaporator stream distributions for the ejector and
541 base compressor suction port.

542 According to the liquid circulation ensured by the liquid ejectors, the vapour quality at the
543 evaporator outlet was assumed to be 0.95. The liquid phase of this stream was drawn by the
544 implemented liquid ejectors from the LPR to the IPR.

545 The same compressor manufacturer was used for the Baseline System and modified
546 installations. However, different types of compressors were utilised for parallel compression
547 purposes due to the higher values of suction pressure. Moreover, on the basis of the auxiliary
548 compressor operating limits, a simulated intermediate pressure (IP) range was assumed.
549 Namely, a simulated 35 bar in the IPR tank was the lowest, and the highest suction pressure
550 was 45 bar.

551 The isentropic efficiency of the base compressors and the parallel compressor was calculated
552 for each simulation on the basis of the data provided from most of the manufacturers. Namely,
553 the power input and heat released are given in certain operating conditions of the condenser and
554 evaporator. According to these data, simple calculations based on the thermodynamic relations
555 for one-stage refrigeration system resulted in the map of the compressors performance. Every
556 of manufacturer's point was used, while the operation between these points were approximated
557 linearly. The efficiency function involved two previously mentioned pressure arguments and
558 was obtained on the basis of the data on the semi-hermetic transcritical CO₂ compressors
559 delivered by the compressor manufacturer [37]. In Fig. 7 and Fig. 8, the isentropic efficiency
560 maps are presented in a function of the high pressure and saturation temperature which
561 correspond to the given pressure level in the evaporator or IPR. The maps ranges were limited
562 to the conditions analysed in the study. Hence, it is not a full range from the manufacturer's
563 website, but only an area needed for the calculations.

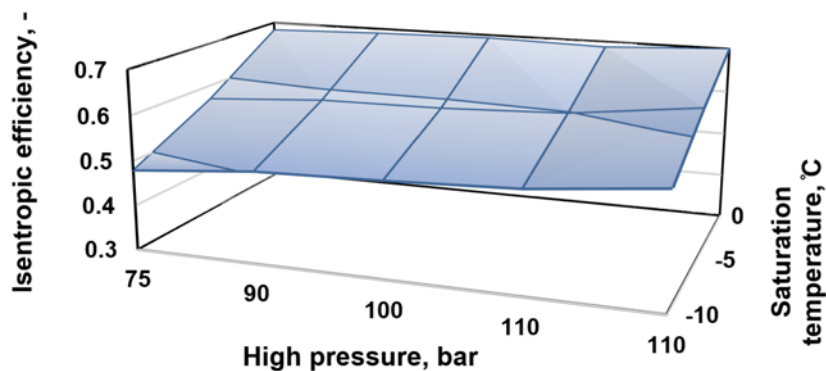


564

565

566

Figure 7. Isentropic efficiency mapped on the basis of the manufacturer's data for subcritical operation.



567

568

569

Figure 8. Isentropic efficiency mapped on the basis of the manufacturer's data for supercritical operation.

570 As mentioned, the performance map available from the manufacturer data was utilised in order
 571 to calculate the compressors efficiency. In this way, the whole range of the assumed pressure
 572 and temperature conditions was covered. Unfortunately, the heat loss data in a full range of the
 573 simulated parameters was not available. Hence, the heat loss would be assumed without any
 574 basis. Moreover, it would be hard to estimate conditions in the fishing vessel machinery due to
 575 still developing R744 technology in the case of such a marine application. Due to that, the heat
 576 loss was neglected in this study. According to this assumption, the temperature at the
 577 compressor outlet was obtained on the basis of the enthalpy calculated from the isentropic
 578 efficiency equation, where values of the isentropic efficiencies were delivered from the
 579 performance maps of the manufacturer used in this study. Having regard small marine
 580 applications, the heat loss from the compressors would be relatively lower when comparing to
 581 the stationary applications with large input powers. Finally, the influence of the isentropic
 582 efficiency onto the specific enthalpy before the gas cooler could be estimated as much more
 583 significant than compressor heat loss [51].

584 On the basis of the compressor manufacturer's data, a superheat of gas at the base compressor
 585 suction port was assumed to have a temperature of 10 K [37]. Equations for the IHX energy
 586 balances were added as well, for which the intermediate heat exchanger efficiency was assumed
 587 to be 100 %.

588 In general, the pressure drops in the R744 system could be evaluated as a relatively low in
589 comparison to those for the synthetic refrigerants as well as for most of the hydrocarbons.
590 Moreover, in the Baseline installation, the lines dimensions were adjusted in order to minimise
591 the pressure drops. Hence, the pressure drops in the Baseline installation are negligible and
592 were not taken into account in this study. Moreover, an evaluation of the other possible pressure
593 drops in the filters, complicated arrangement (due to limited space) of pipelines and in the
594 valves of the whole system (in the form auxiliary equipment of the separators, compressors and
595 ejectors) would be very challenging having regard various conditions of the system work. On
596 the other hand, most of the components mentioned are as compact as possible in order to fit
597 into the restricted areas in the considered marine applications. Consequently, in the cases of the
598 modified installations, the same space limitation could be assumed. Due to that, the specific
599 values of the pressure drops could be evaluated only after a complete design of the installation
600 and its fitting to the fishing boat machinery room. At this stage of the analysis, it would be
601 challenging and simultaneously would influence the results in the minor way due to very
602 advantageous properties of the carbon dioxide.

603 Moreover, some literature reports that the highest pressure drops occur in the evaporator and
604 they are even lower than 1 bar [52]. In this study, the evaporator pressure was iteratively
605 calculated on the basis of the temperature difference between the refrigerant and cooled water.
606 According to a cooled water temperature equal to $-1\text{ }^{\circ}\text{C}$, the required temperature of the
607 refrigerant was calculated as a function of the vapour quality at the evaporator inlet. On the
608 basis of the heat transfer coefficient correlation presented in the work of Cheng [53], a proper
609 function was approximated for vapour quality in the range of .0 to 0.6. The function described
610 the deterioration in the heat transfer conditions with the reduced amount of liquid delivered to
611 the evaporator. Finally, according to the constant evaporator load, the necessary temperature
612 differences were calculated.

613 Cooling capacity was assumed on the basis of control terminal data delivered by the fishing
614 vessel operator. On the basis of the obtained data, the representative evaporator load was
615 estimated at a level of 250 kW, and that value was assumed for all the simulations of heat
616 rejection high temperatures. Moreover, to evaluate possible implementations and amounts of
617 corresponding compressors, the range of evaporator loads was additionally simulated for the
618 case of the most promising solution. That range was assumed to be from 250 kW to 455 kW.

619 To investigate the two mentioned hot climate conditions, two heat rejection temperatures in the
620 gas cooler were assumed. Moreover, the temperature difference between the refrigerant and sea
621 water at the gas cooler outlet was assumed to be 5 K as in the Baseline installation. Hence, 26
622 $^{\circ}\text{C}$ and 38 $^{\circ}\text{C}$ refrigerant temperatures at the outlet of the gas cooler were tested.

623 **4.3. Simulation range for high temperature heat rejection**

624 The input data ranges for the simulations of the modified systems were based on the studies
625 presented by Gullo that focused on the R744 booster system with a parallel compressor [54]
626 [19]. That analysis was based on the optimisation of the high pressure, the temperature at the
627 gas cooler outlet, the parallel compressor mass flow rate and the pressure level in the IPR. In
628 this study, the pressure and temperature ranges presented in Table 1 were investigated. Thus,
629 Mediterranean and East-Asian waters were simulated on the basis of two temperature levels

630 after the gas cooler, and three pressure levels in the IPR were tested. The range of pressure
631 levels in the IPR tank was assumed on the basis of operating limits delivered by the compressor
632 manufacturer [37]. In the work of Gullo, a level of 35 bar was assumed as well. However, those
633 authors assumed that value to be a constant [19]. In this study, three different values were
634 simulated to investigate the influence of this parameter. Finally, for the Mediterranean climate,
635 the high pressure level was tested in the range from 66 bar to 115 bar, where 66 bar is a limit
636 for the subcritical mode. In the case of the East-Asian climate, the pressure at the compressor
637 outlet was simulated in the range from 75 bar to 115 bar. The described parameters were
638 introduced to the model as a set of boundary conditions for the Baseline System and two
639 modified cases (FGV and PC). According to the works of Banasiak [32], Haida [34] and Bodys
640 [35], the intermediate pressures (IP) for the ME systems operating with vapour ejectors were
641 assumed with regard to the multi-ejector module operating range. Hence, the IP were different
642 than for FGV and PC, namely 34 bar, 36 bar and 38 bar. Having regard the configuration based
643 on the combined FGV with PC, the authors defined the scope of the paper in accordance to the
644 state-of-the-art ejector technology. Consequently, the vast majority of the analysis was focused
645 on the multi-ejector system. Hence, the direct analysis of the most perspective solution was
646 chosen by the authors.

647 Table 1. Set of input data for simulations of high temperature heat rejection in Mediterranean
 648 and East-Asian climates.

Climate	Mediterranean	East-Asian
$t_2, ^\circ\text{C}$	26	38
$p_{\text{ipr}}, \text{bar}$	35, 40, 45 (34,36, 38 for ME)	
p_1, bar	66, ..., 115	75, ..., 115

649

650 5. Discussion of the results for the Baseline and modified RSW systems

651 The Baseline System was simulated according to the measurement points of the actual system
 652 under operation. The set of input data and obtained system COP for Baseline System
 653 simulations in Scandinavian conditions are presented in Table 2. The system points are
 654 described in Fig. 1, C1 and C2 denote the frequency settings of compressors 1 and 2,
 655 respectively. \dot{m}_{SUC} denotes the amount of liquid sucked by the ejector in a given system state.
 656 Evaporator load is determined by Q_{EVAP} . The high and low pressure sides of the cycle are given
 657 by p_C and p_O , respectively. According to the state-of-the-art technology discussed in the
 658 literature survey, the positive influence of the liquid ejectors were assumed. Hence, the
 659 experimental data of classic R744 refrigeration unit operating in the marine conditions is not
 660 available. Nevertheless, the reason for the liquid ejector implementation could be found in the
 661 expected performance improvement of the classic R744 system [11]. Five different system
 662 states were simulated on the basis of introduced ejector suction mass flow rate. The first two
 663 states represent the full load state, whereas the other three were related to partial load operation.
 664 According to the lack of motive nozzle measurements, an assumption of a constant MER value
 665 was made to calculate the motive stream. The MER value was assumed to be 1.5 on the basis
 666 of the ejector design process data delivered by SINTEF Energy Research. Moreover, a similar
 667 approach was utilised in the other studies [32], [33], [55]. The level of the obtained system COP
 668 ranged from 4.71 to 9.25. The increments were related to the declining condensation pressure
 669 p_C and increasing suction mass flow rate \dot{m}_{SUC} . Moreover, the relation between condensing
 670 pressure p_C and the declining temperature after condenser t_2 was maintained. The high COP
 671 values provided a wide perspective on further implementation areas. According to the relatively
 672 low values of the condensing pressure and simultaneously lower potential of the recovery work,
 673 the performance of the liquid ejector might be underestimated. On the other hand, in the case
 674 of restricted operating area in the light of the rejection temperatures, i.e. at the Norwegian Coast,
 675 more specialised design of the ejector would be valuable. In this case, a sensitivity study of the
 676 liquid ejector geometry influence on the R744 system operating in low ambient temperatures
 677 could be found as a very useful analysis. However, the actual development of this technology
 678 denotes that the COP improvement is ensured when comparing the classic R744 system layout
 679 and the system equipped in the ejector.

680 Table 2. Input data, data for the Baseline System and obtained COP for an actual RSW
 681 installation operating on the northern Norwegian coast.

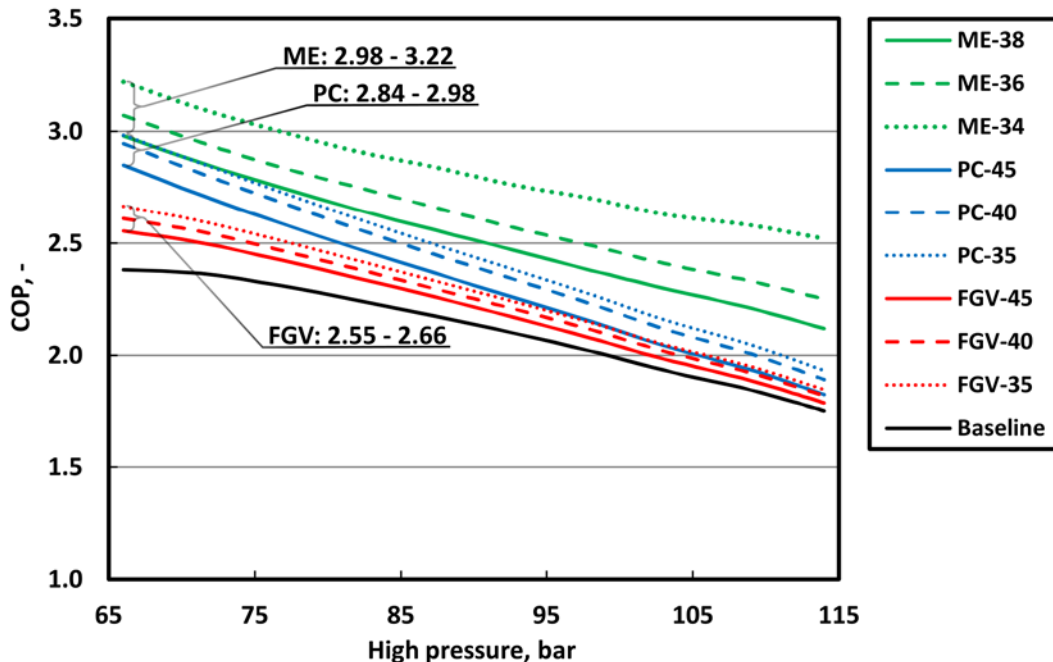
C1	C2	p_c	t_1	t_2	t_3	Q_{EVAP}	\dot{m}_{SUC}	p_o	t_{11}	t_{12}	COP
Hz	Hz	bar	°C	°C	°C	kW	kg/min	bar	°C	°C	-
70	70	55.3	77.3	15.9	1.8	234	0.3	28.3	-6.1	14	4.71
70	70	56.3	70.9	16.5	6.9	353	4.9	30.9	-3.2	14.9	5.34
0	60	50	58.9	12.2	4.8	139	5.7	28.2	-6.2	1.9	5.75
35	35	50.3	64.7	12.5	1.1	144	8.3	28.3	-6.2	12.6	7.65
0	50	48.4	46.9	10.7	4.4	106	6.7	28.4	-6	1.8	9.25

682

683 5.1. Proposed modifications for hot climate applications

684 The Baseline System as well as the modified flash gas valve, parallel compression and multi-
685 ejector systems were tested for the mentioned Mediterranean and East-Asian climates. The
686 results from the first group of simulations (Mediterranean) are presented in Fig. 9, in which the
687 relationship between COP and the high pressure is given. The Baseline System is described by
688 a black curve. The results from FGV, PC and ME are described by the group of red, blue and
689 green curves, respectively. In addition, the value of IP (bar) is indicated by a number after the
690 system determination. The same manner of data presentation was used in further analysis. Some
691 of the parameters were obtained on the basis of modelling assumptions. The evaporator load
692 Q_{EVAP} was set to the constant value of 250 kW. The evaporator pressure p_o was quite constant
693 and between 30.08 bar (-5.5 °C) and 30.28 (-5.1 °C) depending on the vapour/liquid conditions
694 calculated at the evaporator inlet. On the basis of constant efficiency assumed for liquid ejector,
695 the mass entrainment ratio was computed. In the best cases of Mediterranean climate, the values
696 were of 1.8, 1.9 and 0.3 for the FGV, PC and ME system respectively. These relatively high
697 values in the case of FGV and PC are related with low potential of work recovery corresponding
698 to the motive nozzle pressure conditions. In the East-Asian climate, these values become lower
699 due to higher motive nozzle pressures. Namely, they are 0.8, 0.9 and 0.7 for the FGV, PC and
700 ME system, respectively. Finally, the temperature t_2 was 26 °C and 38 °C for the Mediterranean
701 and East-Asian climate, respectively. According to the temperature assumed for the
702 Mediterranean climate, the R744 systems should work in the subcritical mode. Hence, the
703 obtained character of the curves shows that the optimum pressure is located at the lowest
704 possible value. Further increment of the high-side pressure results in the additional compressor
705 work with insufficiently enough increment of the cooling capacity. This subcritical mode can
706 be compared to the others refrigerant with high temperatures of the critical point. According to
707 the results presented in Fig. 9, the highest COP, 3.22, is related to the ME system and 34 bar in
708 the IPR, namely for case ME-34. Increasing pressure in the IPR deteriorated the COP of the
709 ME system, which is related to the too small amount of recovered work in the ejector. Having
710 considered the higher motive pressure (gas cooler pressure), the ratio of the COP decrement
711 decreased. An explanation is found in the higher potential for work recovery available in the
712 ejector in the region of higher pressures. Nevertheless, in the case of the highest COP, the
713 efficiency for ME was only on a slightly lower level than that of the Baseline System under
714 favourable Scandinavian conditions. A similar situation is related to the FGV and PC systems.

715 Namely, the lowest pressure in the IPR provided the highest performance based on the increased
 716 cooling capacity. Regarding the FGV and PC systems, the obtained COPs were at a lower level
 717 than that for the ME systems. For the lowest pressure related to the operating limits of the
 718 subcritical mode, the PC and FGV systems ensured COP of 2.98 and 2.66, respectively. Due to
 719 this, the lowest possible level of high pressure should be ensured for optimal performance.

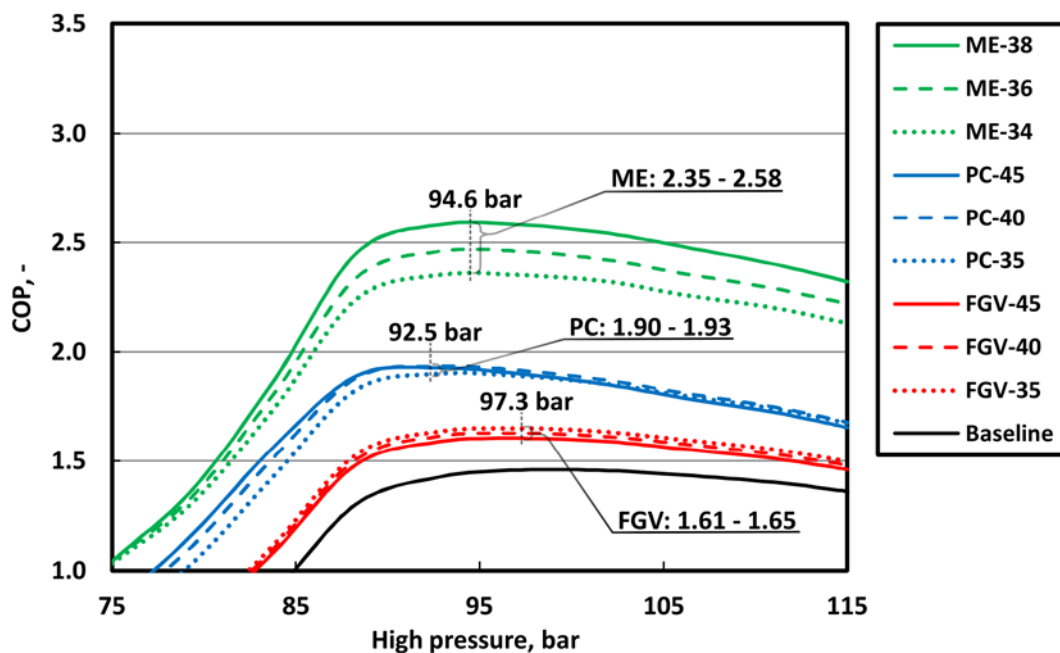


720
 721 Figure 9. COP of the Baseline System and the modified cases presented as a function of high
 722 pressure from simulations performed for the Mediterranean climate.

723 Simulation cases of the heat rejection temperature characteristic for East-Asian waters provided
 724 the results presented in Fig. 10 in the same manner case identification was used for Fig. 9.
 725 However, in Fig. 10, the optimum pressure of each system is marked by a vertical line with the
 726 corresponding pressure value. Having regard higher temperature of the heat rejection which is
 727 above the CO₂ critical point, the character of the curves is substantially different comparing to
 728 Fig. 9. The reasons are located in the supercritical state of operation. Consequently, the
 729 condenser should be exchanged into a gas cooler because the heat rejection takes place above
 730 the critical point. This change is characteristic for R744 and brings several aspects to consider.

731 First of all, a wide range of optimum operations should be seen due to small changes in
 732 performance near optimum pressure. However, significant differences are visible between the
 733 performances of each system. Namely, the best prospective solution is related to the ME system,
 734 for which the maximum COP is equal to 2.58 at 94.6 bar of high side pressure. The optimum
 735 pressure in the IPR is different than for the lower heat rejection temperatures, and a higher ME
 736 system performance was obtained in the case of the highest pressure in the IPR tank. This
 737 relation is directly connected with the increasingly efficient operation of the multi-ejector
 738 module delivering the vapour to higher pressure levels. Simultaneously, higher pressure levels
 739 at the parallel compressor suction port directly result in lower power consumptions. However,
 740 the difference between the investigated IP is on the level of 5 % - the highest COP of ME-36 is
 741 equal to 2.46, whereas that for the mentioned ME-38 is 2.58. Moreover, the differences between

742 system COP are more visible for various IP of the ME system than for the PC and FGV systems.
 743 The latter ones seem to be much less dependent on pressure in the IPR. Increasing high pressure
 744 delivers a quite visible better performance of mentioned 40 bar of the IP, which is related to the
 745 balance between recovered work and the favourable conditions of parallel compressor work. In
 746 the FGV case, even the smaller difference is visible, and the other trend is obtained as well. The
 747 FGV system should operate in the lowest IP throughout the range to obtain the highest
 748 performance, with a COP of 1.65. Regarding an optimum high side pressure, slightly different
 749 values were obtained for each system, which is related to other factors of crucial impact on
 750 system COP. In the case of ME, it is the ejector efficiency and the performance of the parallel
 751 compressor. In the case of the PC and FGV systems, the final results are created at an optimum
 752 point between parallel compressor efficiency and amount of gas in the IPR tank. The
 753 computations for the PC system resulted in the highest COP for a high side pressure of 92.5 bar
 754 in the PC configuration. Concerning the series of curves related to FGV, the optimal COP value
 755 was obtained at system high side pressure levels of approximately 97 bar. The global trends of
 756 every simulated system can be described as being similar. However, the modified systems are
 757 characterised by significant COP differences one to another, especially in the range of optimal
 758 pressures after the compressors. Moreover, different pressures for optimal operation should be
 759 ensured for each case, and the PC optimum should be reached for the lowest pressure in
 760 comparison to the other systems.



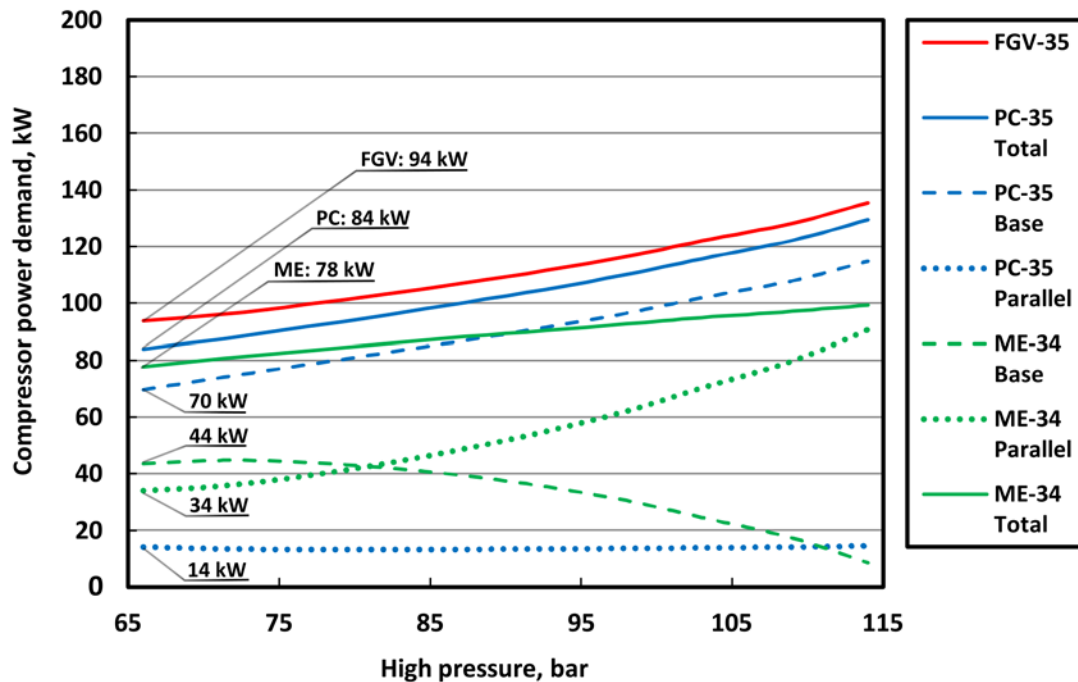
761
 762 Figure 10. COP of the Baseline System and the modified cases presented as a function of high
 763 pressure from simulations performed for the East-Asian climate.

764 **5.2. System modifications according to power demand increment**

765 According to the goals, possible modifications were analysed in the light of the restricted spatial
 766 volumes in the machinery rooms of fishing vessels. From this perspective, the most demanding
 767 system would be a ME or PC unit due to the additional compressor implementation. However,
 768 under the higher ambient conditions (East-Asian), in the ME unit only the parallel compressors

769 could be applied to circulate the refrigerant; this will be further explained below. Moreover,
770 regarding the obtained COP improvements of the modified systems, the ME was assigned as
771 the most promising solution. Nevertheless, due to the higher ambient (sea water) temperatures
772 compared with those for Scandinavian conditions, higher power consumptions are expected. In
773 the Baseline System configuration, two base compressors characterised by a maximum power
774 of 44 kW are used [37]. The maximum power of the transcritical CO₂ compressors available
775 from the manufacturer used in this study is approximately 58.3 kW [37]. To avoid introducing
776 a third compressor into the fishing vessel machinery room, two compressors with a maximum
777 power demand of 58.3 kW should be used for the purposes of PC. To evaluate these
778 possibilities, an analysis of compressor power and corresponding system efficiency is provided.

779 Requirements on compressor power for the Mediterranean and East-Asian climates are
780 presented in Fig. 11 and Fig. 12, respectively. The total compressor power for FGV is presented
781 as a function of the high side pressure (red line). The ME (green) and the PC (blue) systems are
782 represented by solid, dashed and dotted lines for their total power consumptions, base load
783 compressors and parallel compressors, respectively. The same manner of case determination
784 was used for the graph presented in Fig. 12. According to Fig. 9, the point of optimal operation
785 is related to the lowest pressure, where the power consumption is at the lowest level. Operation
786 of the FGV system can be obtained by two compressors of similar maximum power to obtain
787 approximately 94 kW of total power at the optimal (lowest) high pressure. Moreover, the total
788 work of each compressor could be on a level from below 58.3 kW up to approximately 90 bar.
789 In the case of the more advanced solutions, lower power consumption is presented. However,
790 despite that, one additional compressor should be delivered for the PC solution to cover parallel
791 compression purposes. This is caused by the very low consumption of the parallel compressor
792 and the high, increasing power of the base compressor section, which exceeds the assumed
793 maximum power of one compressor - 58.3 kW. Hence, in the Mediterranean climate, the same
794 set of compressors as in the Baseline system can be used only in the case of the FGV and ME
795 configurations. Nevertheless, the low COP of the FGV system should disqualify such an
796 implementation. The difference in required powers of FGV and ME is significant, and only the
797 ME system should be considered. In the case of the ME system, similar compressors for base
798 and parallel purposes should be used with a proper modification of the piping system. Finally,
799 the required maximum power of compressors installed in the Baseline System would be enough
800 for the Mediterranean climate, whereas the ME system would ensure the most efficient
801 operation.

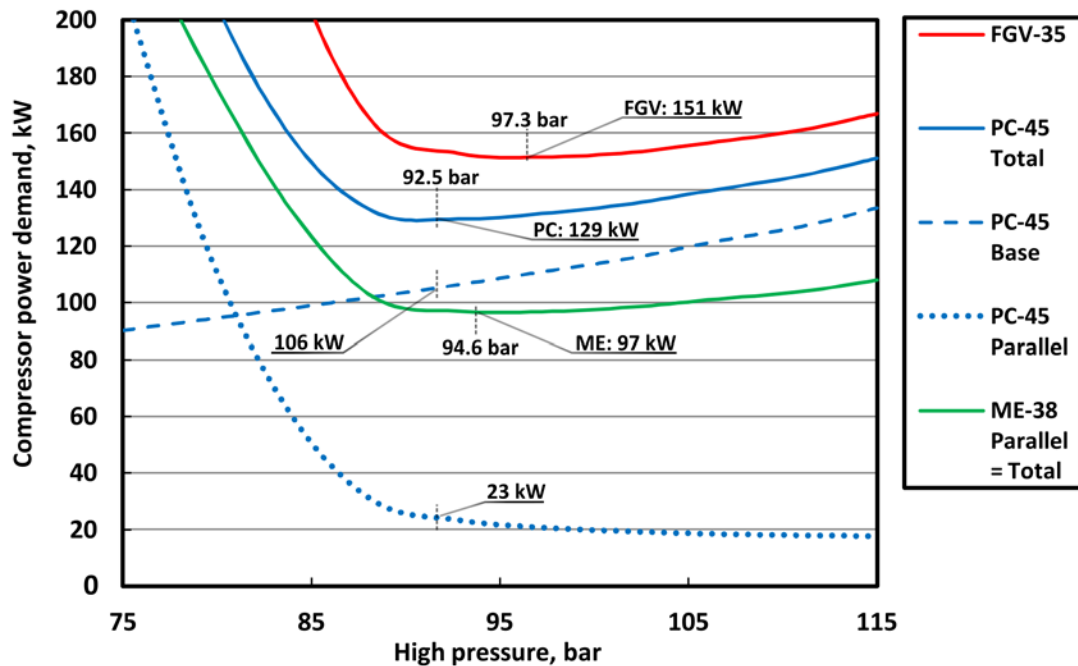


802

803 Figure 11. Compressor power demand of the modified systems characterised by the highest
 804 COP improvement in Mediterranean climate.

805 The power consumption for the East-Asian climate is characterised by definitely higher values
 806 than for the Mediterranean climate. Moreover, a non-linear trend is presented in Fig. 12, in
 807 which the power consumption results are described in the same manner as in Fig. 11. First,
 808 significantly more power is needed in the case of a FGV or PC unit. In comparison with the
 809 power consumption for the Mediterranean climate, approximately 60 % and 53 % more energy
 810 should be delivered for FGV and PC operating in an East-Asian climate. In the same
 811 comparison, the ME system operating under East-Asian conditions needs only 24 % more
 812 power. Due to the mentioned necessary power, a FGV system could not operate without an
 813 additional third compressor because the FGV total power (151 kW) is significantly higher than
 814 the 115 kW corresponding to two compressors. The base compressor section of the PC system
 815 would be covered by two compressors. However, only a very narrow buffer of additional
 816 cooling capacity would be ensured. Namely, the mentioned maximum power for two
 817 compressors is approximately 115 kW, whereas the base compressors of the PC system would
 818 operate at a level of 106 kW. On the other hand, any significant additional cooling load would
 819 be impossible to obtain in such an installation. Moreover, parallel compression could be
 820 employed by an additional third compressor of 23 kW. Thus, under these conditions, FGV and
 821 PC systems would require one additional compressor. Finally, the ME unit provides the only
 822 solution without the necessity of an additional third compressor. In this approach, the base load
 823 compressor is totally unloaded by the multi-ejector module. Hence, all of the refrigerant vapour
 824 from the evaporator could be delivered to higher pressures, applying the ejectors as a booster
 825 for the parallel compressors. The required power of the ME-unit would be at a level of 97 kW.
 826 The obtained reduced power consumption is based on the large amount of potential work
 827 recovery and the elevated pressure level at the parallel compressors' suction port and its high
 828 isentropic efficiency based on the low pressure ratio. Moreover, partially increased cooling

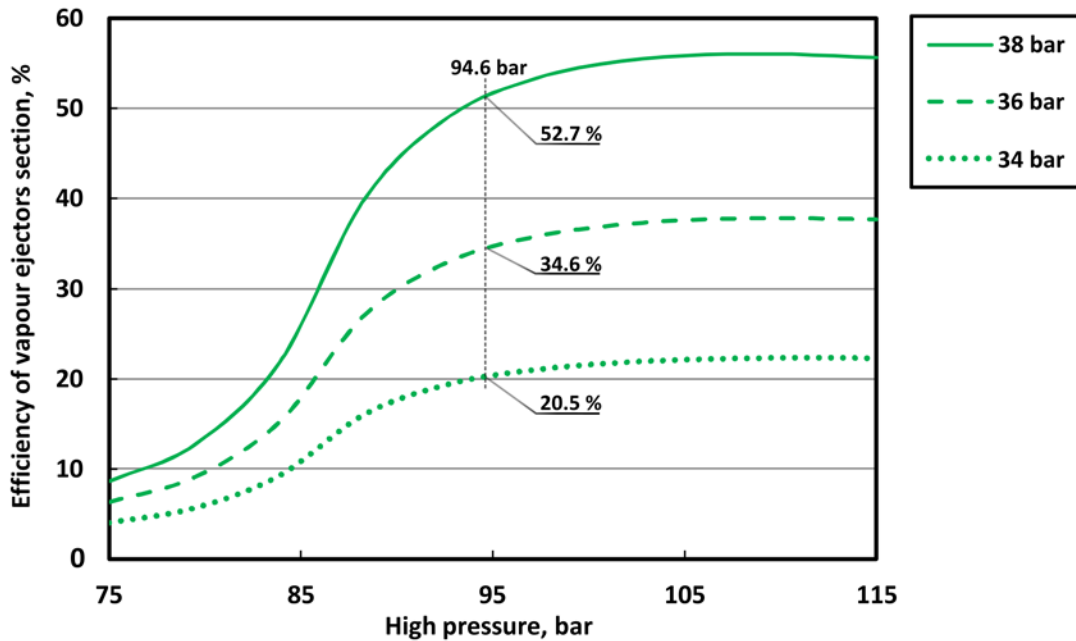
829 capacity is ensured by liquid ejectors. As a final result, only two compressors of 58.3 kW would
 830 be enough to ensure operation of the R744 refrigeration unit in an East-Asian climate.



831
 832 Figure 12. Compressor power demands of the modified systems characterised by the highest
 833 COP improvement for the East-Asian climate.

834 5.3. Ejector efficiency requirements in an East-Asian climate

835 In the case of the East-Asian climate, the system was modelled as utilizing parallel compressors
 836 only. Consequently, the entire evaporator stream was ingested by the vapour ejectors of a multi-
 837 ejector module. Due to that, the necessary efficiencies of the vapour ejector section to operate
 838 under the given conditions were calculated on the basis of the definition proposed by Elbel and
 839 Hrnjak [33]. In Fig. 13, the ejector efficiency obtained for each pressure in the IPR is presented.
 840 According to the COP data presented in Fig. 10, optimum pressure is marked to point to the
 841 necessary efficiency of the vapour ejector section. First, a significant difference between
 842 efficiencies is visible for higher pressures, including the range of optimum pressures. Having
 843 considered the data presented in the literature, efficiencies of vapour ejectors on the level of 35
 844 % could be estimated as the highest reported [32]. Therefore, operation at a pressure level of
 845 36 bar in the IPR tank could be stated as possible at this moment in vapour ejector development.
 846 Nevertheless, in the case of the highest IP, a significant improvement in ejector technology
 847 should be provided to reach the level of 52 % efficiency. The potential for significant
 848 improvements in efficiency up to a level of 45 % was described in previous work by the authors
 849 of this study [35]. In the case of the efficiency mentioned, the IP should be maintained on the
 850 level of 37.17 bar. On the other hand, as discussed, the COP difference between ME-36 and
 851 ME-38 is on the level of 5 %. Hence, the ME-36 performance remains at a high level
 852 comparable to that for ME-38.



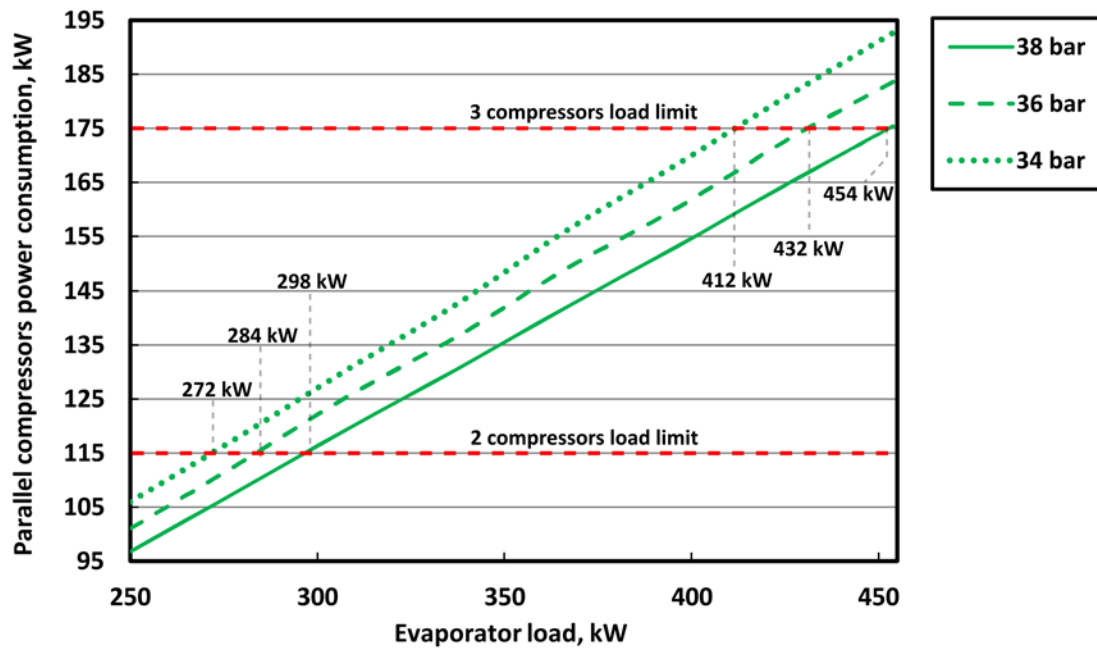
853

854 Figure 13. The required efficiency of the vapour ejector section in the multi-ejector module
 855 for each of the investigated pressures in the IPR.

856

5.4. Available cooling load in the function of installed compressor power

857 The assumed cooling load of 250 kW could be described as being representative for
 858 Scandinavian operation. Having regarded the various amounts and kinds of catches, different
 859 evaporator loads might be obtained. The necessary powers for the ME system as a function of
 860 evaporator load are presented in Fig. 14. The simulations were performed for optimum
 861 operation under East-Asian conditions. The maximum power for a single compressor was
 862 assumed on the basis of the manufacturer's data [37]. According to the limit of utilizing two
 863 compressors, evaporator loads ranging from 272 kW to 298 kW could be obtained depending
 864 on IP, which is directly related to ejector efficiency. This range is wider for higher capacities
 865 when differences between operations with higher or lower IPRs are more significant. On the
 866 other hand, three compressors could deliver a significantly higher evaporator load than two
 867 compressors. Namely, in the least efficient scenario of 34 bar, available cooling capacity would
 868 be on the level of approximately 412 kW. Hence, in an installation equipped with a third
 869 compressor, approximately 52 % of additional available evaporator load would be ensured.
 870 Moreover, in the case of the mentioned high efficiency multi-ejector module and 38 bar of IP,
 871 the increment of available evaporator load can even reach 67 %.



872

873 Figure 14. Necessary power for parallel compressors in the ME system operating at optimum
874 pressure as a function of evaporator load.

875 6. Conclusions and further work

876 A mathematical model of the classic R744 refrigeration unit equipped with the liquid ejector
877 was developed and utilised to evaluate performance of the installation operating in a fishing
878 vessel in Scandinavian conditions.

879 On the basis of data obtained from NASA Earth Observatory online databases [41],
880 Mediterranean and East-Asian sea waters were simulated for heat rejection temperatures of 21
881 °C and 33 °C, respectively. According to the thermodynamic characteristics of R744, system
882 modifications were necessary to maintain high system performance. Nevertheless, spatial
883 limitations of the fishing vessel machinery room required the additional consideration of
884 introduced equipment related to the modified systems.

885 Simulations of East-Asian conditions resulted in the other trend of the COP distribution. First,
886 significant differences were presented between each of the tested configurations. Again, the
887 most prospective solution was ME, where the maximum obtained COP was 2.58. In the
888 investigated configurations, the optimal high pressure was approximately 95 bar. Moreover, the
889 range of high performance could be described as being relatively wide according to the high
890 pressure value. That characteristic should provide advantages in regulation and automation
891 areas. Substantial benefits could be found in the field due to the minimised requirements on
892 equipment space.

893 East-Asian, which offered more demanding conditions, showed only one proper solution in the
894 form of ME. In this case, as for the Mediterranean climate, a third compressor is not necessary.
895 However, two compressors of higher power input should be delivered for parallel compression.

896 In the case of the analysed highest heat rejection temperatures, results in the form of necessary
897 vapour ejector section efficiency were obtained. According to the operation with parallel

898 compressors only, the entire stream from the evaporator was consumed by the vapour ejectors.
899 According to literature data, ejectors of the demanded efficiency can be designed for two of the
900 three investigated IP pressures - 34 bar and 36 bar. To obtain a higher system efficiency on the
901 basis of an IP of 38 bar, improved vapour ejectors would be necessary. However, this efficiency
902 increment could be described as relatively high for next generation ejectors. Finally, the results
903 showed good prospects for higher cooling capacities according to the implementation of the
904 third compressor.

905 According to the main goal of the paper, the analysis for the marine application with
906 refrigeration system equipped in the liquid ejector was presented and more efficient solution
907 for hot ambient conditions was proposed for such a system. Hence, the system analysis was
908 performed having regard overall performance of the cycle. Nevertheless, the presented
909 investigation was focused on the possibilities related with the multi-ejector system. A strong
910 relation between the ejector technology and refrigeration system was discussed in Section 5.2
911 and especially in Section 5.3. Despite the global character of the analysis, the presented range
912 of the promising operation for ejectors in a certain configuration and the specified efficiency
913 seems to describe this solution as a very universal from the considered application point of
914 view. Moreover, consequence of the ejector technology is illustrated as a substantial reduction
915 of space requirements in the limited area of machinery room at the fishing vessel. Finally, the
916 maintaining of the required cooling capacity without additional equipment as well as possible
917 additional buffer related with only one additional compressor was obtained.

918 **Acknowledgments**

919 The content and main goals of the paper were formulated according to a partnership with
920 Kuldeteknisk AS. The work of JB and JS was partially supported by SUT Rector research grants
921 08/060/RGJ18/0158 and 08/060/RGP17/0135, respectively as well as by the statutory research
922 fund of the Faculty of Power and Environmental Engineering, Silesian University of
923 Technology.

924 **References**

- 925 [1] United Nations Environment Programme (UNEP), “Montreal Protocol,” 1987.
926 [2] United Nations Framework Convention on Climate Change (UNFCCC), “Kyoto
927 Protocol,” 1997.
928 [3] European Commission, “Regulation (EU) No 517/2014 of the European Parliament and
929 of the Council of 16 April 2014 on fluorinated greenhouse gases and repealing
930 Regulation (EC) No 842/2006 Text with EEA relevance,” *Off. J. Eur. Union*, vol. 57,
931 pp. 195–230, 2014.
932 [4] American Society of Heating Refrigerating and Air-Conditioning Engineers,
933 *ANSI/ASHRAE Standard 34, Designation and Safety Classification of Refrigerants*.
934 Atlanta, GA, USA: ASHRAE, 2016.
935 [5] M. D. Hurley, T. J. Wallington, M. S. Javadi, and O. J. Nielsen, “Atmospheric chemistry
936 of CF₃CF=CH₂: Products and mechanisms of Cl atom and OH
937 radical initiated oxidation,” *Chem. Phys. Lett.*, vol. 450, no. 4–6, pp. 263–267, 2008.
938 [6] T. Imamura, K. Kamiya, and O. Sugawa, “Ignition hazard evaluation on A2L refrigerants
939 in situations of service and maintenance,” *J. Loss Prev. Process Ind.*, vol. 36, pp. 553–

- 940 561, 2015.
- 941 [7] A. Mota-Babiloni, J. Navarro-Esbri, A. Barragan-Cervera, F. Moles, and B. Peris,
942 “Analysis based on EU Regulation No 517 / 2014 of new HFC / HFO mixtures as
943 alternatives of high GWP refrigerants in refrigeration and HVAC systems,” *Int. J.*
944 *Refrig.*, vol. 52, pp. 21–31, 2015.
- 945 [8] Z. Jin, T. M. Eikevik, P. Nekså, A. Hafner, and R. Wang, “Annual energy performance
946 of R744 and R410A heat pumping systems,” *Appl. Therm. Eng.*, vol. 117, pp. 568–576,
947 2017.
- 948 [9] G. Lorentzen, “Revival of carbon dioxide as a refrigerant,” *Int. J. Refrig.*, vol. 17, no. 5,
949 pp. 292–301, 1994.
- 950 [10] O. Joneydi Shariatzadeh, S. S. Abolhassani, M. Rahmani, and M. Ziaee Nejad,
951 “Comparison of transcritical CO₂ refrigeration cycle with expander and throttling valve
952 including/excluding internal heat exchanger: Exergy and energy points of view,” *Appl.*
953 *Therm. Eng.*, vol. 93, pp. 779–787, 2016.
- 954 [11] G. Lorentzen, “The use of natural refrigerants: a complete solution to the CFC/HCFC
955 predicament,” *Int. J. Refrig.*, vol. 18, no. 3, pp. 190–197, 1995.
- 956 [12] IPU & Department of Mechanical Engineering of Technical University of Denmark,
957 “CoolPack; ISO 817:2014; EN 378-1:2008.” 2017.
- 958 [13] A. Hafner, S. Försterling, and K. Banasiak, “Multi-ejector concept for R-744
959 supermarket refrigeration,” *Int. J. Refrig.*, vol. 43, pp. 1–13, 2014.
- 960 [14] A. Polzot, P. D’Agaro, and G. Cortella, “Energy Analysis of a Transcritical CO₂
961 Supermarket Refrigeration System with Heat Recovery,” *Energy Procedia*, vol. 111, no.
962 September 2016, pp. 648–657, 2017.
- 963 [15] K. M. Tsamos, Y. T. Ge, I. Santosa, S. A. Tassou, G. Bianchi, and Z. Mylona, “Energy
964 analysis of alternative CO₂ refrigeration system configurations for retail food
965 applications in moderate and warm climates,” *Energy Convers. Manag.*, p. In Press:
966 dx.doi.org/10.1016/j.enconman.201, 2017.
- 967 [16] A. Hafner, “R744 train HVAC unit,” in *12th IIR Gustav Lorentzen Conference*, 2016, p.
968 Paper ID: 1132.
- 969 [17] S. Minetto, L. Cecchinato, R. Brignoli, S. Marinetti, and A. Rossetti, “Water-side
970 reversible CO₂ heat pump for residential application,” *Int. J. Refrig.*, vol. 63, pp. 237–
971 250, 2016.
- 972 [18] J. Ignacio, A. Villarino, and F. Ángel, “Experimental and modelling analysis of an office
973 building HVAC system based in a ground-coupled heat pump and radiant floor,” *Appl.*
974 *Energy*, vol. 190, pp. 1020–1028, 2017.
- 975 [19] P. Gullo, G. Cortella, S. Minetto, and A. Polzot, “Overfed Evaporators and Parallel
976 Compression in Commercial R744 Booster Refrigeration Systems – an Assessment of
977 Energy Benefits,” in *12th IIR Gustav Lorentzen Natural Working Fluids Conference*,
978 2016, p. Paper ID: 1039.
- 979 [20] B. Y. K. De Carvalho, C. Melo, and R. H. Pereira, “A Study on the Use of Liquid
980 Separators in Variable-Speed Small-Scale Carbon Dioxide Refrigerating Sytems,” in
981 *12th IIR Gustav Lorentzen Natural Working Fluids Conference*, 2016, p. Paper ID: 1014.
- 982 [21] A. Mota-Babiloni, P. Makhnatch, and R. Khodabandeh, “Recent investigations in HFCs
983 substitution with lower GWP synthetic alternatives: focus on energetic performance and

- 984 environmental impact,” *Int. J. Refrig.*, p. In Press:
 985 doi.org/10.1016/j.ijrefrig.2017.06.026, 2017.
- 986 [22] J. Sarkar and N. Agrawal, “Performance optimization of transcritical CO₂ cycle with
 987 parallel compression economization,” *Int. J. Therm. Sci.*, vol. 49, no. 5, pp. 838–843,
 988 2010.
- 989 [23] Y. Ruan, Q. Liu, Z. Li, and J. Wu, “Optimization and analysis of Building Combined
 990 Cooling, Heating and Power (BCHP) plants with chilled ice thermal storage system,”
 991 *Appl. Energy*, vol. 179, pp. 738–754, 2016.
- 992 [24] A. Farsi, S. M. H. Mohammadi, and M. Ameri, “An efficient combination of transcritical
 993 CO₂ refrigeration and multi- effect desalination: Energy and economic analysis,”
 994 *Energy Convers. Manag.*, vol. 127, pp. 561–575, 2016.
- 995 [25] K. Manjunath, O. P. Sharma, S. K. Tyagi, and S. C. Kaushik, “Thermodynamic analysis
 996 of a supercritical/transcritical CO₂ based waste heat recovery cycle for shipboard power
 997 and cooling applications,” *Energy Convers. Manag.*, vol. 155, pp. 262–275, Jan. 2018.
- 998 [26] A. D. Akbari and S. M. S. Mahmoudi, “Thermoeconomic performance and optimization
 999 of a novel cogeneration system using carbon dioxide as working fluid,” *Energy Convers.*
 1000 *Manag.*, vol. 145, pp. 265–277, Aug. 2017.
- 1001 [27] S. Elbel and N. Lawrence, “Review of recent developments in advanced ejector
 1002 technology,” *Int. J. Refrig.*, vol. 62, pp. 1–18, 2016.
- 1003 [28] T. Bai, J. Yu, and G. Yan, “Advanced exergy analyses of an ejector expansion
 1004 transcritical CO₂ refrigeration system,” *Energy Convers. Manag.*, vol. 126, pp. 850–861,
 1005 2016.
- 1006 [29] Y. Zhu, C. Li, F. Zhang, and P.-X. Jiang, “Comprehensive experimental study on a
 1007 transcritical CO₂ ejector-expansion refrigeration system,” *Energy Convers. Manag.*, vol.
 1008 151, pp. 98–106, Nov. 2017.
- 1009 [30] L. Zheng, J. Deng, and Z. Zhang, “Dynamic simulation of an improved transcritical CO₂
 1010 ejector expansion refrigeration cycle,” *Energy Convers. Manag.*, vol. 114, pp. 278–289,
 1011 2016.
- 1012 [31] C. Lucas and J. Koehler, “Experimental investigation of the COP improvement of a
 1013 refrigeration cycle by use of an ejector,” *Int. J. Refrig.*, vol. 35, no. 6, pp. 1595–1603,
 1014 Sep. 2012.
- 1015 [32] K. Banasiak *et al.*, “Development and performance mapping of a multi-ejector expansion
 1016 work recovery pack for R744 vapour compression units,” *Int. J. Refrig.*, vol. 57, pp. 265–
 1017 276, 2015.
- 1018 [33] S. Elbel and P. Hrnjak, “Experimental validation of a prototype ejector designed to
 1019 reduce throttling losses encountered in transcritical R744 system operation,” *Int. J.*
 1020 *Refrig.*, vol. 31, no. 3, pp. 411–422, 2008.
- 1021 [34] M. Haida, K. Banasiak, J. Smolka, A. Hafner, and T. M. Eikevik, “Experimental analysis
 1022 of the R744 vapour compression rack equipped with the multi-ejector expansion work
 1023 recovery module,” *Int. J. Refrig.*, vol. 64, no. August, pp. 93–107, 2016.
- 1024 [35] J. Bodys *et al.*, “Full-scale multi-ejector module for a carbon dioxide supermarket
 1025 refrigeration system: Numerical study of performance evaluation,” *Energy Convers.*
 1026 *Manag.*, vol. 138, pp. 312–326, Apr. 2017.
- 1027 [36] G. Boccardi, F. Botticella, G. Lillo, R. Mastrullo, A. W. Mauro, and R. Trinchieri,

- 1028 “Experimental investigation on the performance of a transcritical CO₂ heat pump with
1029 multi-ejector expansion system,” *Int. J. Refrig.*, p. In Press:
1030 doi.org/10.1016/j.ijrefrig.2017.06.013, 2017.
- 1031 [37] GEA, “VAP for Stationary Applications - version 11.4.2 (online),”
1032 <http://vap.gea.com/stationaryapplication/Pages/Index.aspx>, 2017. [Online]. Available:
1033 <http://vap.gea.com/stationaryapplication/Pages/Index.aspx>. [Accessed: 01-Jun-2017].
- 1034 [38] C.-C. Wang, A. Hafner, C.-S. Kuo, and W.-D. Hsieh, “An overview of the effect of
1035 lubricant on the heat transfer performance on conventional refrigerants and natural
1036 refrigerant R-744,” *Renew. Sustain. Energy Rev.*, vol. 16, no. 7, pp. 5071–5086, Sep.
1037 2012.
- 1038 [39] Andrei Tronin, “The satellite-measured sea surface temperature change in the Gulf of
1039 Finland,” *Int. J. Remote Sens.*, vol. 38, no. 6, pp. 1541–1550, 2017.
- 1040 [40] A. Sakalli, “Sea surface temperature change in the mediterranean sea under climate
1041 change: A linear model for simulation of the sea surface temperature up to 2100,” *Appl.*
1042 *Ecol. Environ. Res.*, vol. 15, no. 1, pp. 707–716, 2017.
- 1043 [41] NASA Earth Observation (NEO), “Sea Surface Temperature (MODIS),” 2017. [Online].
1044 Available: <https://neo.sci.gsfc.nasa.gov/>. [Accessed: 20-Jun-2017].
- 1045 [42] F-Chart Software, “Engineering Equations Solver (EES).” Middleton, WI, USA, 2016.
- 1046 [43] F. Liu and E. A. Groll, “Analysis of a Two Phase Flow Ejector For Transcritical CO₂
1047 Cycle,” 2008.
- 1048 [44] K. Banasiak and A. Hafner, “1D Computational model of a two-phase R744 ejector for
1049 expansion work recovery,” *Int. J. Therm. Sci.*, vol. 50, no. 11, pp. 2235–2247, Nov. 2011.
- 1050 [45] F. Liu and E. A. Groll, “Study of ejector efficiencies in refrigeration cycles,” *Appl.*
1051 *Therm. Eng.*, vol. 52, no. 2, pp. 360–370, Apr. 2013.
- 1052 [46] H. Zhang, L. Wang, L. Jia, and X. Wang, “Assessment and prediction of component
1053 efficiencies in supersonic ejector with friction losses,” *Appl. Therm. Eng.*, vol. 129, pp.
1054 618–627, Jan. 2018.
- 1055 [47] M. E. Ahammed, S. Bhattacharyya, and M. Ramgopal, “Thermodynamic design and
1056 simulation of a CO₂ based transcritical vapour compression refrigeration system with an
1057 ejector,” *Int. J. Refrig.*, vol. 45, pp. 177–188, Sep. 2014.
- 1058 [48] M. Nakagawa, a. R. Marasigan, T. Matsukawa, and a. Kurashina, “Experimental
1059 investigation on the effect of mixing length on the performance of two-phase ejector for
1060 CO₂ refrigeration cycle with and without heat exchanger,” *Int. J. Refrig.*, vol. 34, no. 7,
1061 pp. 1604–1613, Nov. 2011.
- 1062 [49] L. Zheng and J. Deng, “Research on CO₂ ejector component efficiencies by experiment
1063 measurement and distributed-parameter modeling,” *Energy Convers. Manag.*, vol. 142,
1064 pp. 244–256, Jun. 2017.
- 1065 [50] A. B. Little and S. Garimella, “A critical review linking ejector flow phenomena with
1066 component- and system-level performance,” *Int. J. Refrig.*, vol. 70, pp. 243–268, Oct.
1067 2016.
- 1068 [51] IPU Refrigeration and Energy Engineering, “CO₂ plant.” Kgs. Lyngby, Denmark, 2012.
- 1069 [52] P. Gullo, G. Cortella, and S. Minetto, “Potential Enhancement Investigation of
1070 Commercial R744 Refrigeration Systems Based on Avoidable and Unavoidable Exergy

- 1071 Destruction Concepts,” in *12th IIR Gustav Lorentzen Natural Working Fluids*
1072 *Conference*, 2016, no. 2014.
- 1073 [53] L. Cheng, G. Ribatski, L. Wojtan, and J. R. Thome, “New flow boiling heat transfer
1074 model and flow pattern map for carbon dioxide evaporating inside horizontal tubes,” *Int.*
1075 *J. Heat Mass Transf.*, vol. 49, no. 21–22, pp. 4082–4094, Oct. 2006.
- 1076 [54] P. Gullo, B. Elmegaard, and G. Cortella, “Energy and environmental performance
1077 assessment of R744 booster supermarket refrigeration systems operating in warm
1078 climates,” *Int. J. Refrig.*, vol. 64, pp. 61–79, 2016.
- 1079 [55] M. Haida *et al.*, “Numerical investigation of an r744 liquid ejector for supermarket
1080 refrigeration systems,” *Therm. Sci.*, vol. 20, no. 4, pp. 1259–1269, 2016.
- 1081